

QC  
807.5  
.U6  
F7  
no.28  
c.2

Technical Memorandum OAR FSL-28



---

## RUC20 – THE 20-KM VERSION OF THE RAPID UPDATE CYCLE

S.G. Benjamin  
J.M. Brown  
K.J. Brundage  
D. Dévényi  
G.A. Grell  
D. Kim  
B. E. Schwartz  
T.G. Smirnova  
T.L. Smith  
S.S. Weygandt  
G.S. Manikin

Forecast Systems Laboratory  
Boulder, Colorado  
July 2002



QC  
807.5  
.46  
F7  
no. 28  
c. 2

NOAA Technical Memorandum OAR FSL-28

## RUC20 – THE 20-KM VERSION OF THE RAPID UPDATE CYCLE

S.G. Benjamin

J.M. Brown

K.J. Brundage

D. Dévényi

G.A. Grell

D. Kim

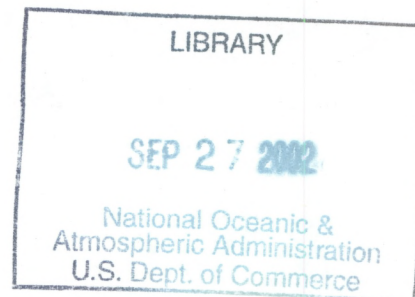
B. E. Schwartz

T.G. Smirnova

T.L. Smith

S.S. Weygandt

NOAA Forecast Systems Laboratory, Boulder, Colorado



G.S. Manikin

NOAA Environmental Modeling Center, National Centers for Environmental Prediction,  
Camp Springs, Maryland

Forecast Systems Laboratory

Boulder, Colorado

July 2002



**UNITED STATES  
DEPARTMENT OF COMMERCE**

**Donald L. Evans  
Secretary**

**NATIONAL OCEANIC AND  
ATMOSPHERIC ADMINISTRATION**

**VADM Conrad C. Lautenbacher, Jr.  
Under Secretary for Oceans  
and Atmosphere/Administrator**

**Oceanic and Atmospheric  
Research Laboratories**

**David L. Evans  
Director**



## NOTICE

Mention of a commercial company or product does not constitute an endorsement by the NOAA Oceanic and Atmospheric Research Laboratories. Use of information from this publication concerning proprietary products or the test of such products for publicity or advertising purposes is not authorized.

---

For sale by the National Technical Information Service, 5285 Port Royal Road  
Springfield, VA 22061



## Contents

<u>Section</u>	<u>Page</u>
Abstract.....	1
1. Introduction.....	3
2. Spatial Resolution.....	3
2.1 Horizontal resolution.....	5
2.2 Vertical resolution.....	7
3. Forecast Model Changes in RUC20.....	9
3.1 Basic dynamics/numerics.....	9
3.2 Physical parameterizations.....	10
3.2.1 Explicit mixed-hase cloud/moisture processes.....	10
3.2.2 Convective parameterization.....	11
3.2.3 Land-surface physics.....	13
3.2.4 Atmospheric radiation.....	15
3.2.5 Turbulent mixing.....	15
3.2.6 Time splitting for physical parameterization.....	15
4. Changes to Lateral and Lower Boundary Conditions in RUC20.....	16
4.1 Lateral boundary conditions.....	16
4.2 Lower boundary conditions.....	16
5. Analysis Changes in RUC20.....	18
5.1 Assimilation of GOES cloud-top pressure data.....	18
5.2 Improved observation preprocessing.....	19
5.3 Modifications to optimal interpolation analysis.....	20
6. RUC20 Output Files and Variables.....	21
6.1 Output files.....	21
6.2 Changes to GRIB identifiers for RUC20.....	21
6.3 Basic 3-D output variables.....	22
6.4 RUC 2-D diagnosed variables.....	22
7. Statistical Verification Against Rawinsondes.....	25
8. References.....	26
Appendix A: Known or suspected RUC20 biases or deficiencies.....	28
Appendix B: Comments from field users during RUC20 evaluation.....	28



## RUC20 – The 20-km Version of the Rapid Update Cycle

Stanley G. Benjamin, John M. Brown, Kevin J. Brundage, Dezső Dévényi,  
Georg A. Grell, Dongsoo Kim, Barry E. Schwartz, Tatiana G. Smirnova,  
Tracy Lorraine Smith, Stephen S. Weygandt, and Geoffrey S. Manikin

**Abstract.** A major revision to the Rapid Update Cycle (RUC) analysis/model system was implemented into operations at the National Centers for Environmental Prediction Center (NCEP) on 17 April 2002. The new RUC version with 20-km horizontal resolution (RUC20) replaces the previous 40-km version of the RUC (RUC40).

### Summary of RUC20 vs. RUC40 (RUC-2) differences

**Horizontal resolution:** The RUC20 has a 20-km horizontal resolution, compared to 40 km for the previous RUC40 (RUC-2). The area covered by the computational grid has not changed. The RUC20 has a 301x225 horizontal grid, compared to 151 x 113 for the RUC40.

**Vertical resolution:** The RUC20 has 50 computational levels, compared to 40 levels for the RUC40, and continues to use the hybrid isentropic-sigma vertical coordinate as in previous versions of the RUC.

**Improved moist physics:** Improved quantitative precipitation forecasts have been the primary focus for changes in the RUC20 model, including a major revision in the MM5/RUC mixed-phase microphysics cloud routine, and a new version of the Grell convective parameterization with an ensemble approach to closure and feedback assumptions. The main effect of the microphysics change is to decrease overforecasting of graupel and ice and improve the precipitation type forecast. The new Grell scheme provides in considerable improvement in convective precipitation forecasts from the RUC.

**Assimilation of GOES cloud-top data:** The RUC20 includes a cloud analysis that updates the initial three-dimensional (3-D) cloud/hydrometeor fields by combining cloud-top pressure data from GOES with the background 1-h RUC hydrometeor field. Cloud clearing and building is done to improve the initial cloud water/ice/rain/snow/graupel fields for the RUC.

**Better use of observations in analysis:** The RUC20 assimilates near-surface observations more effectively through improved algorithms for calculating observation-background differences. Assimilation of surface observations is improved by diagnosing background forecasts for surface temperature and dewpoint at 2 m and for winds at 10 m. It is also improved by matching land-use type between the background and the observation for near-coastal stations. The RUC20 continues to use an optimal interpolation analysis as in the RUC40 – implementation of a 3-D variational analysis has been deferred.

**Improved land-surface physics:** The RUC20 land-surface model is changed from that of the RUC40. It uses more detailed land-use and soil texture data, in contrast to 1-degree resolution fields used in the RUC40. It includes improved cold-season processes (soil freezing/thawing) and a two-layer snow model. These changes improve the evolution of surface moisture and temperature and snow cover, which in turn improve forecasts of surface temperature and moisture and precipitation.



**Lateral boundary conditions:** The RUC40 used lateral boundary conditions specified from the Eta model initialized every 12 h. The RUC20 adds updates of its lateral boundaries from the 0600 and 1800 UTC Eta runs.

**Improved postprocessing:** The RUC20 includes improved diagnostic techniques for 2-m temperature and dewpoint, 10-m winds, helicity, visibility, convective available potential energy, and convective inhibition.

**Most significant improvements in RUC20 fields over those from RUC40 (RUC-2).**

- **Precipitation (both summer and winter)** – From improved precipitation physics and higher resolution
- **All surface fields (temperature, moisture, winds)** – Reduced bias and RMS error in comparison with METAR observations. From improved surface and cloud/precipitation physics and higher resolution
- **Upper-level winds and temperatures** – From higher vertical and horizontal resolution, better physics
- **Orographically induced precipitation and circulations** – From higher horizontal resolution, cloud physics, and better use of surface data near mountains.



## 1. INTRODUCTION

A new version of the Rapid Update Cycle (RUC) has been implemented at the National Centers for Environmental Prediction (NCEP) on 17 April 2002 with a doubling of horizontal resolution (40 km to 20 km), an increased number of vertical computational levels (40 to 50), and improvements in the analysis and model physical parameterizations. A primary goal in development of the 20-km RUC (or RUC20) has been improvement in warm-season and cold-season quantitative precipitation forecasts. Improvements in near-surface forecasts and cloud forecasts have also been targeted. The RUC20 provides improved forecasts for these variables, as well as for wind, temperature, and moisture above the surface.

The RUC20 provides improved short-range numerical weather guidance for general public forecasting as well as for the special short-term needs of aviation and severe-weather forecasting. The RUC20 continues to produce new analyses and short-range forecasts on an hourly basis, with forecasts out to 12 h run every 3 h. The implementation of the RUC20 in 2002 follows previous major implementations of a 60-km 3-h cycle version in 1994 (Benjamin et al. 1994, 1991) and a 40-km 1-h cycle version in 1998 (Benjamin et al. 1998).

The uses of the RUC summarized below continue with the RUC20:

- **Explicit use of short-range forecasts** – The RUC forecasts are unique in that they are initialized with very recent data. Thus, usually, the most recent RUC forecast has been initialized with more recent data than other available NCEP model forecasts. Even at 0000 or 1200 UTC, when other model runs are available, the RUC forecasts are useful for comparison over the next 12 h. Although there are many differences between the RUC and other NCEP models, the key unique aspects of the RUC are its hybrid isentropic vertical coordinate (used in the analysis and model), hourly data assimilation, and model physics.
- **Monitoring current conditions with hourly analyses** – Hourly analyses are particularly useful when overlaid with hourly satellite and radar images, or hourly observations such as from surface stations or profilers.
- **Evaluating trends of longer-range models** – RUC analyses and forecasts are useful for evaluation of the short-term predictions of the Eta and AVN models.

The users of the RUC include:

- Aviation Weather Center/NCEP, Kansas City, MO
- Storm Prediction Center/NCEP, Norman, OK
- NWS Weather Forecast Offices
- FAA/DOT, including use for air traffic management and other automated tools, and for FAA workstations
- NASA Space Flight Centers
- Private sector weather forecast providers

Sections below describe changes in the RUC with the RUC20 implementation regarding spatial resolution, data assimilation, model, changes to lower and lateral boundary condition, and diagnostics/postprocessing. Known or suspected RUC biases or deficiencies as of April 2002 (per FSL) are shown in Appendix A. Comments from a field test for the RUC20 held March and April 2002 are included in Appendix B.

## 2. SPATIAL RESOLUTION

The RUC20 occupies the same spatial domain as the previous RUC40 (40-km RUC-2), as shown in Figs. 1a,b. The RUC20 grid points are still a subset of the AWIPS Lambert conformal grid (AWIPS/GRIB grid 215 for 20 km) used as a distribution grid by the National Weather Service. Direct use of the AWIPS grid reduces the number of distribution grids for the RUC. The AWIPS grid ID for the RUC20 grid is 252, compared to 236 for the RUC40 grid. Thus, the 252 grid for the RUC20 is a subset of the 215 grid, and the RUC20 grid size is 301 x 225 grid points (compared to 151 x 113 for RUC40).



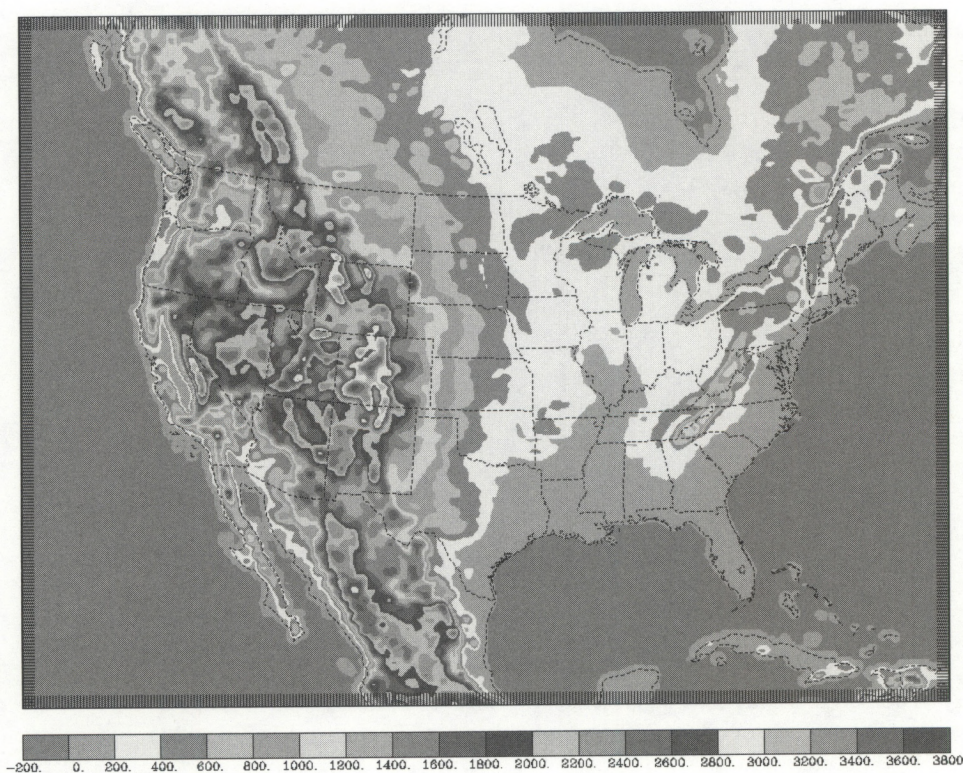
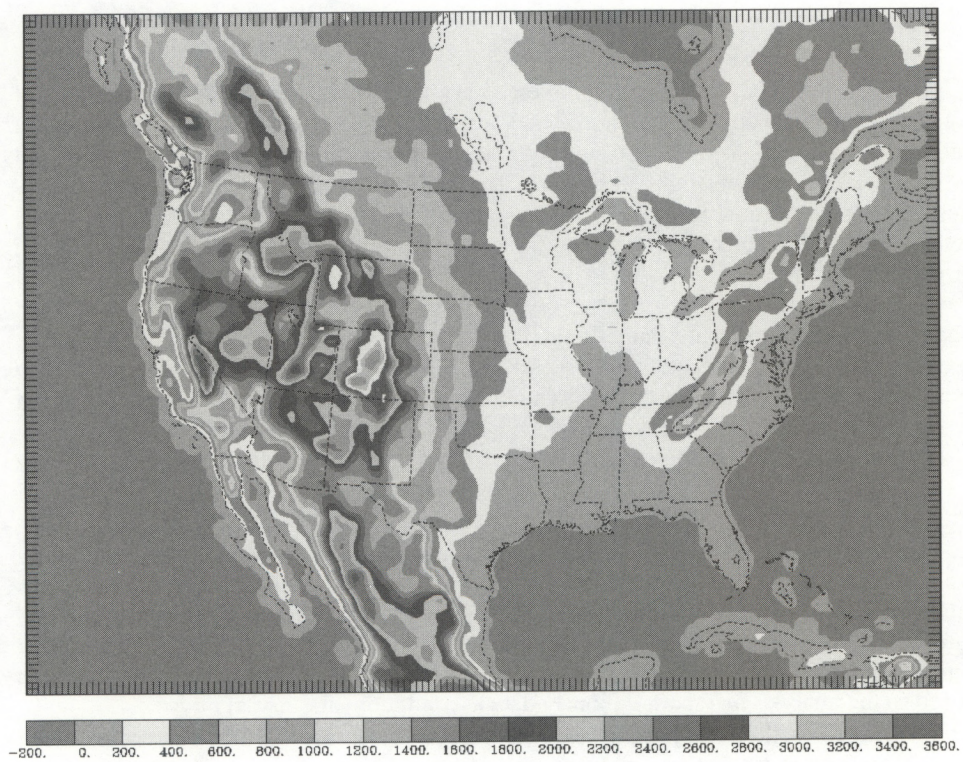


**Figure 1. Terrain elevation for a) (above) 40-km RUC-2, b) (below) 20-km RUC20.**



## 2.1. Horizontal resolution

The 20-km grid spacing allows better resolution of small-scale terrain variations, leading to improved forecasts of many topographically induced features, including low-level eddies, mountain/valley circulations, mountain waves, sea/lake breezes, and orographic precipitation. It also allows better resolution of land-water boundaries and other land-surface discontinuities. While the most significant differences in the terrain resolution of the RUC20 (Fig. 1b) vs. RUC40 (Fig. 1a) are in the western United States, a number of important differences are also evident in the eastern part of the domain.

The surface elevation of the RUC20, as in the RUC40, is defined as a "slope envelope" topography. The standard envelope topography is defined by adding the sub-grid-scale terrain standard deviation (calculated from a 10-km terrain field) to the mean value over the grid box. By contrast, in the slope envelope topography, the terrain standard deviation is calculated with respect to a plane fit to the high-resolution topography within each grid box. This gives more accurate terrain values, especially in sloping areas at the edge of high-terrain regions. It also avoids a tendency of the standard envelope topography to project the edge of plateaus too far laterally onto low terrain regions. Using the slope envelope topography gives lower terrain elevation at locations such as Denver and Salt Lake City, which are located close to mountain ranges. As shown in Table 1, the RUC20 more closely matches station elevations in the western United States.

The grid length is 20.317 km at 35 deg N. Due to the varying map-scale factor from the projection, the actual grid length in RUC20 decreases to as small as 16 km at the north boundary. The grid length is about 19 km at 43 deg N. The RUC20 latitude/longitude (and terrain elevation) at each point in an ASCII file can be downloaded from <http://ruc.fsl.noaa.gov/MAPS.domain.html>. The lower left corner point is (1,1), and the upper right corner point is (301,225), as shown in Table 2.

**Table 1. Terrain elevation difference between station elevation and interpolated RUC elevation for selected rawinsonde stations in western United States.**

Rawinsonde station	Station elevation minus RUC40 elevation (m)	Station elevation minus RUC20 elevation (m)
Edwards AFB, CA	300	41
Denver, CO	354	26
Grand Junction, CO	679	323
Boise, ID	274	253
Great Falls, MT	157	29
Reno, NV	381	144
Elko, NV	352	152
Medford, OR	544	346
Salem, OR	233	51
Rapid City, SD	153	45
Salt Lake City, UT	630	438
Riverton, WY	225	119



**Table 2. Latitude/longitude and AWIPS-212 positions of corner points for the RUC20 domain.**

RUC20 point	AWIPS-212 point	Latitude	Longitude
(1,1)	(23,7)	16.2810 N	126.1378 W
(1,225)	(23,119)	54.1731 N	139.8563 W
(301,1)	(173,7)	17.3400 N	69.0371 W
(301,225)	(173,119)	55.4818 N	57.3794 W

An example is shown below (Fig. 2) of the improved orographic effect on low-level wind circulation comparing 3-h forecasts from RUC20 and RUC40, both displayed at 40-km resolution. The RUC20 shows a better depiction of the Denver-area cyclonic circulation, strong southerly flow up the San Luis Valley into southern Colorado near Alamosa, and winds of greater than 20 knots near higher terrain in central Colorado and south central Utah. The verifying analysis in Fig. 3 shows that all of these features appear to be better depicted in the RUC20 3-h forecasts.

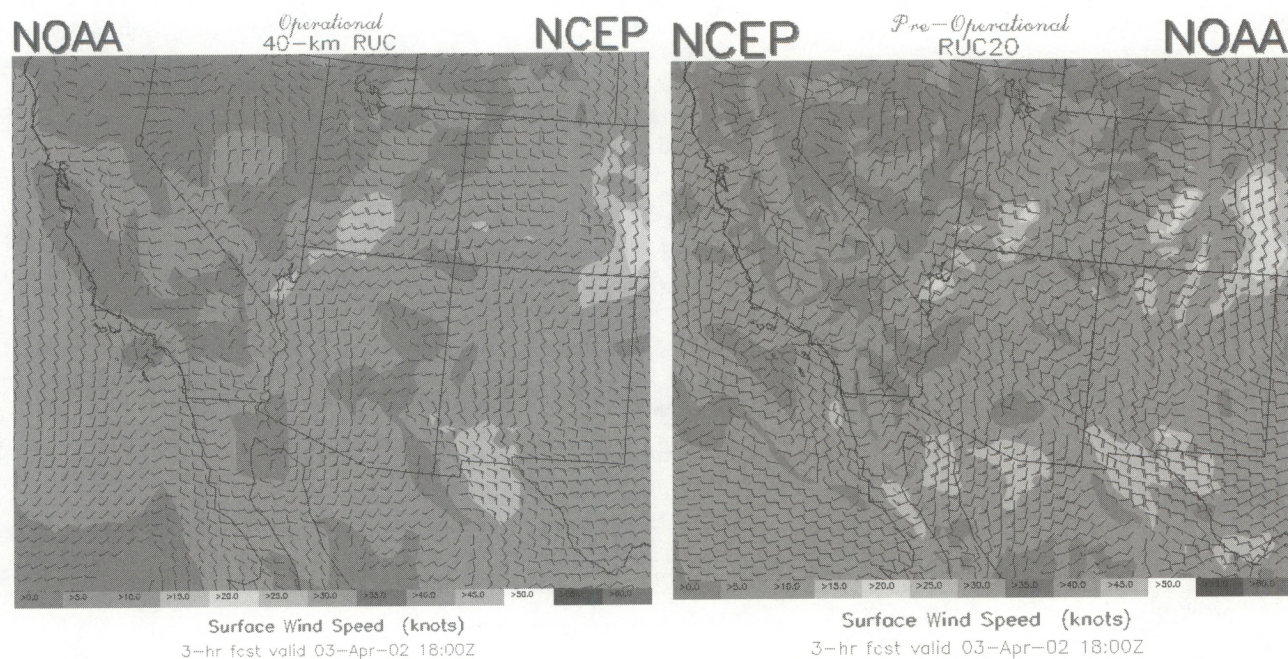


**Figure 2. RUC 3-h surface wind forecasts from a) (left) RUC40 and b) (right) RUC20. Forecasts valid at 1800 UTC 3 April 2002.**



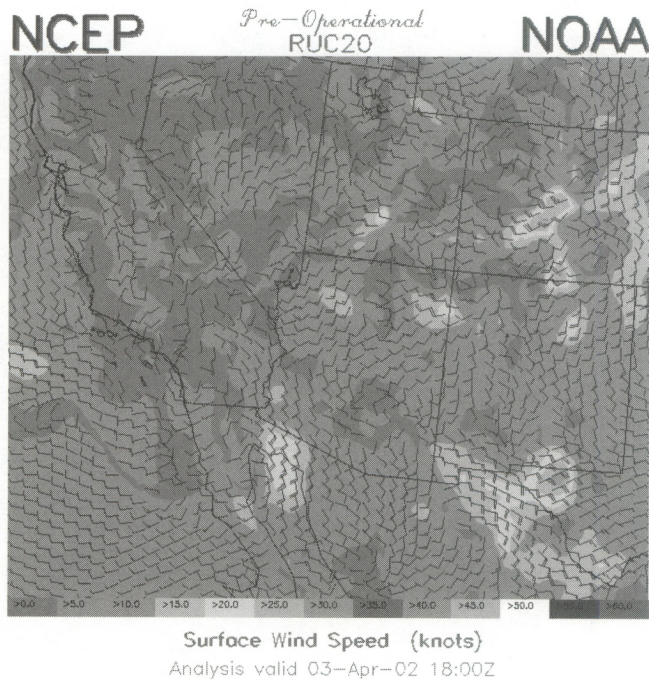


**Figure 3. Verifying analysis of surface winds at 1800 UTC 3 April 2002 from RUC20.**

## 2.2 Vertical resolution

The RUC20 continues to use the generalized vertical coordinate configured as a hybrid isentropic-sigma coordinate (Bleck and Benjamin 1993) used in previous versions of the RUC. This coordinate is used for both the analysis and the forecast model. The RUC hybrid coordinate has terrain-following layers near the surface with isentropic layers above. This coordinate has proven to be advantageous in providing sharper resolution near fronts and the tropopause (e.g., Benjamin 1989, Johnson et al. 1993, 2000). Some of the other advantages are:

- All of the adiabatic component of the vertical motion on the isentropic surfaces is captured in flow along the 2-D surfaces. Vertical advection through coordinate surfaces, which usually has somewhat more truncation error than horizontal advection, is less prominent in isentropic/sigma hybrid models than in quasi-horizontal coordinate models. This characteristic results in improved moisture transport and less precipitation spin-up problem in the first few hours of the forecast.
- Improved conservation of potential vorticity. The potential vorticity and tropopause level (based on the 2.0 PV unit surface) show very good spatial and temporal coherence in RUC grids (Olsen et al 2000).
- Observation influence in the RUC analysis extends along isentropic surfaces, leading to improved air-mass integrity and frontal structure. From an isobaric perspective, the RUC isentropic analysis is implicitly anisotropic (Benjamin 1989).

The RUC20 has 50 vertical levels, compared to 40 levels in RUC40. Extra levels are added near the tropopause and lower stratosphere and also in the lower troposphere. The RUC hybrid coordinate is defined as follows:

- Each of the 50 levels is assigned a reference virtual potential temperature ( $\theta_v$ ) that increases upward (Table 3).
- The lowest atmospheric level ( $k=1$ ) is assigned as the pressure at the surface (the model terrain elevation).
- Each of the next 49 levels is assigned a minimum pressure thickness between it and the next level below. This thickness will apply to coordinate surfaces in the lower portion of the domain where the coordinate surfaces are terrain-following. For grid points with surface elevation near sea level, the minimum pressure thickness is 2.5, 5.0, 7.5, and 10 hPa for the bottom 4 layers, and 15 hPa for all layers above. These minimum pressure thicknesses are reduced over higher terrain to avoid bulges of sigma layers protruding upward in these regions.

- The pressure corresponding to the reference  $\theta_v$  for each ( $k$ ) level is determined for each ( $i,j$ ) column. (For lower  $\theta_v$  values, this pressure may be determined via extrapolation as beneath the ground.)

- At this point, there are two choices for the assignment of pressure to the ( $i,j,k$ ) grid point, corresponding to:



- 1) the reference  $\theta_v$  value (the *isentropic* definition), and
  - 2) the minimum pressure spacing, starting at the surface pressure (the *sigma* definition)
- If the isentropic pressure (1) is less than sigma pressure (2), the grid point pressure is defined as isentropic, or otherwise as terrain-following (sigma).

**Table 3. Reference  $\theta_v$  values (K) for the RUC20 (50 levels).**

224	232	240	245	250	255	260	265	270	273
276	279	282	285	288	291	294	296	298	300
302	304	306	308	310	312	314	316	318	320
322	325	328	331	334	337	340	343	346	349
352	355	359	365	372	385	400	422	450	500

The maximum  $\theta_v$  value in the RUC20 is 500 K, compared to 450 K for the RUC40. The 500 K surface is typically found at 45-60 hPa. As with the RUC40, a greater proportion of the hybrid levels are assigned as terrain-following in warmer regions and warmer seasons. This is shown in Figs. 4a,b below.

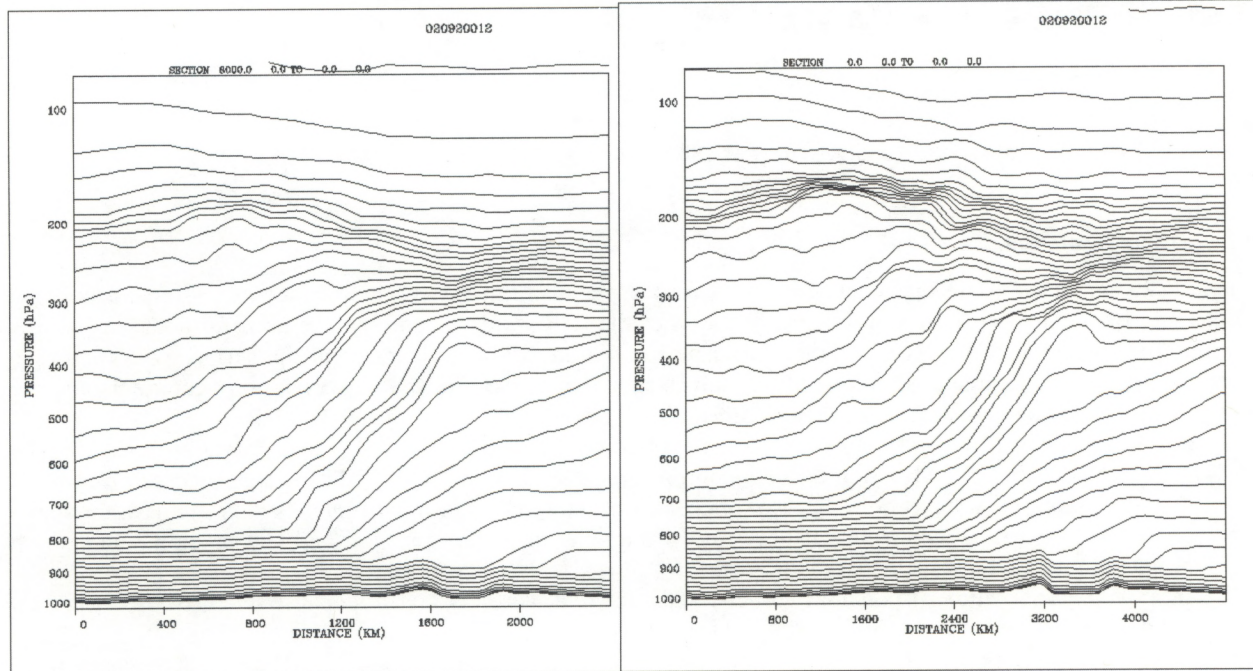


**Figure 4. Vertical cross sections showing RUC native coordinate levels for a) (left) RUC40 — 40 levels, and b) (right) RUC20 — 50 levels. Data are taken from RUC 12-h forecasts valid at 1200 UTC 2 April 2002. Cross sections are oriented from south (Mississippi) on left to north (western Ontario) on right.**

In this example (Fig. 4), north-south vertical cross sections are shown depicting the pressure at which the RUC native levels are found for a particular case. The case shown is from April 2002, with the cross section extending from Mississippi (on the left) northward through Wisconsin (center point), across Lake Superior (slightly higher terrain on each side), and ending in western Ontario. A frontal zone is present in the middle of the cross section, where the RUC levels (mostly isentropic) between 700 and 300 hPa are strongly sloped.



In the RUC20, seven new levels have been added with reference  $\theta_v$  values between 330 K and 500 K. Three new levels with reference  $\theta_v$  in the 270–290 K range have also been added. In the RUC20 depiction (Fig. 4b), the tropopause is more sharply defined than in the RUC40, and there are more levels in the stratosphere, resulting from the additional levels in the upper part of the domain. In the RUC20, the isentropic levels from 270–355 K are now resolved with no more than 3-K spacing.

### 3. FORECAST MODEL CHANGES IN RUC20

The RUC20 forecast model is similar to that for the RUC40 but with important changes in physical parameterizations and smaller changes in numerical approaches. The model continues to be based upon the generalized vertical coordinate model described by Bleck and Benjamin (1993). Modifications to a 20-line section of code in the model are sufficient to modify it from the hybrid isentropic-sigma coordinate described in section 2.2 to either a pure sigma or pure isentropic model.

#### 3.1 Basic dynamics/numerics

First, the basic numerical characteristics of the RUC model are reviewed (*italicized where different in the RUC20 from the RUC40*).

- Arakawa-C staggered horizontal grid (Arakawa and Lamb 1977); *u and v horizontal wind points offset from mass points to improve numerical accuracy.*
- Generalized vertical coordinate equation set and numerics for adiabatic part of model following Bleck and Benjamin (1993)
- No vertical staggering.
- *Time step is 30 seconds at 20-km resolution.*
- Positive definite advection schemes used for continuity equation (advection of pressure thickness between levels) and for horizontal advection (Smolarkiewicz 1983) of virtual potential temperature and all vapor and hydrometeor moisture variables.
- Application of adiabatic digital filter initialization (DFI, Lynch and Huang 1992) for 40-min period forward and backward before each model start. The use of the DFI in the RUC is important for producing a sufficiently “quiet” (reduced gravity wave activity) 1-h forecast to allow the 1-h assimilation cycle. *A problem in application of digital filter weights is corrected in the RUC20.*

The atmospheric prognostic variables of the RUC20 forecast model are:

- pressure thickness between levels
- virtual potential temperature -  $\theta_v$
- horizontal wind components
- water vapor mixing ratio
- cloud water mixing ratio
- rain water mixing ratio
- ice mixing ratio
- snow mixing ratio
- graupel (rimed snow, frozen rain drops) mixing ratio
- number concentration for ice particles
- turbulence kinetic energy

The soil prognostic variables (at six levels) of the RUC forecast model are:

- soil temperature
- soil volumetric moisture content

Other surface-related prognostic variables are snow water equivalent moisture and snow temperature (*at 2 layers in RUC20*), and canopy water.

Other differences in the RUC20 vs. RUC40 model numerics or design are as follows:

- The order of solution in each time step:

RUC40	RUC20
Continuity	Continuity
Horizontal advection of $\theta_v$ / moisture	Horizontal advection of $\theta_v$ / moisture
Physics (sub-grid-scale parameterizations)	Physics
Coordinate adjustment	Momentum
Momentum	Coordinate adjustment

- The vertical advection for all variables is now calculated in a consistent manner using upstream differencing. The placement of the call for coordinate adjustment at the end of the time step allows this consistent treatment.
- More robust and flexible hybrid coordinate algorithm
- Much improved modularization
- *Use of new version of Scalable Modeling System (SMS) message-passing library with nonintrusive compiler directives (Govett et al. 2001) and improved modularization led to a significant reduction in lines of code in the RUC20 model.*

### 3.2 Physical parameterizations

#### 3.2.1 Explicit mixed-phase cloud/moisture processes.

The RUC20 uses an updated version (Brown et al 2000) of the explicit microphysics from the NCAR/Penn State MM5 mesoscale model MM5 (level 4, Reisner et al. 1998). An earlier version of this scheme was also used in the RUC40. This scheme explicitly predicts mixing ratios for five hydrometeor species – cloud water, rain water, snow, ice, graupel and also the ice particle number concentration. This explicit mixed-phase prediction is different than the diagnostic mixed-phase prediction used in the Eta-12. In the RUC model, all six cloud/hydrometeor variables are advected horizontally using the positive definite scheme of Smolarkiewicz (1983) on the isentropic-sigma levels with adaptive vertical resolution and advected vertically using upstream differencing (see section 3.1). The hydrometeor variables cycled without modification in the RUC40 1-h cycle are modified by GOES cloud-top pressure assimilation in the RUC20, as described in section 4.

Significant changes to the RUC/MM5 microphysics (Brown et al. 2000) have been introduced with the RUC20. These changes address unreasonable behavior in the RUC40 regarding excessive graupel and lower than expected amounts of supercooled liquid water. The modifications, developed jointly by NCAR and FSL, include a different curve for ice nucleation as a function of temperature (Cooper replacing Fletcher), new assumed particle size distributions for graupel to reduce the number of small particles, a modified procedure for graupel formation as a result of riming of cloud ice, and revisions to the calculation of cloud-ice particle number concentration. These modifications have been successful in reducing excessive graupel (e.g., Fig. 5) and in improving the precipitation-type forecast (less sleet) in the RUC20.



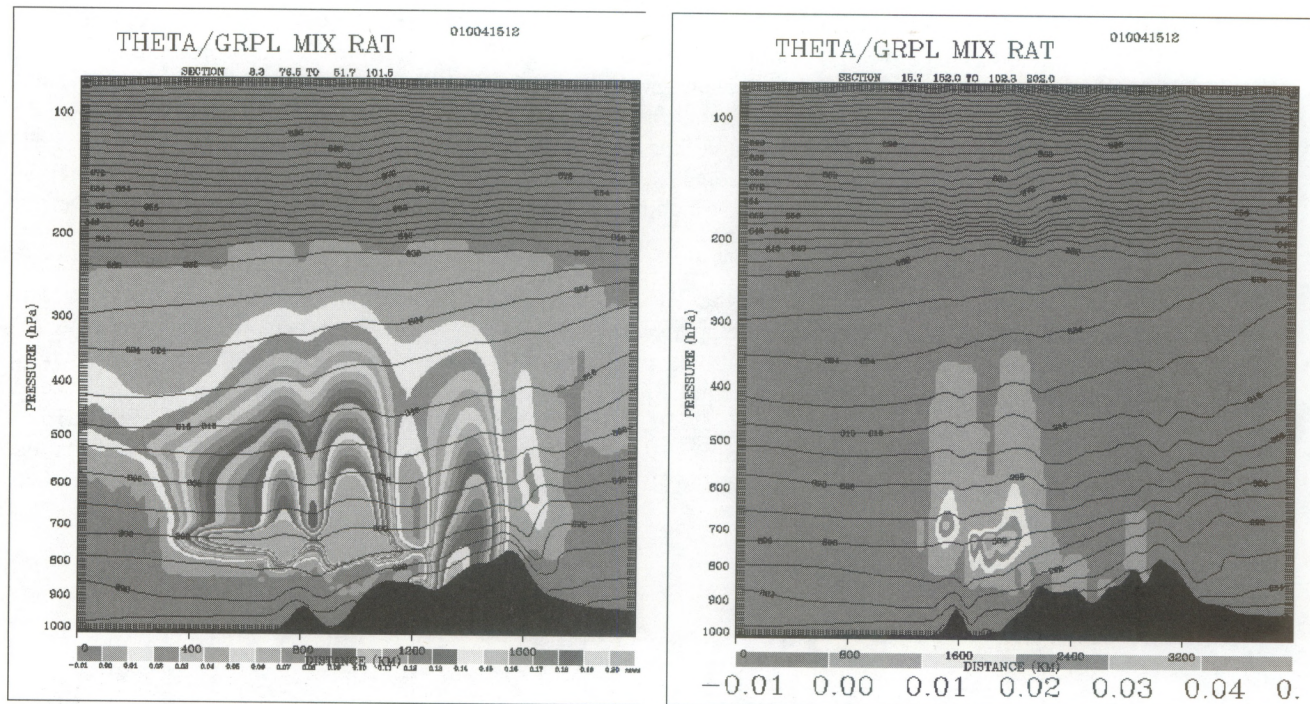


Figure 5. Graupel and potential temperature in vertical cross sections from a) (left) RUC40 and b) (right) RUC20. For 12-h forecasts valid 0300 UTC 5 January 2001. Cross section is oriented SW (left) to NE (right) across Washington (Olympic Peninsula) into British Columbia and Alberta.

### 3.2.2 Convective parameterization

A new convective parameterization (Grell and Devenyi 2001) based on an ensemble approach is used in the RUC20. This scheme is based on the Grell (1993) scheme but draws on other schemes by using an ensemble of various closure assumptions. The version of the Grell/Devenyi scheme used in the RUC20 includes the following closures:

$$\frac{\partial(\text{CAPE})}{\partial t}$$

- $\frac{\partial(\text{CAPE})}{\partial t}$ , where CAPE is convective available potential energy
- removal of total CAPE (Kain and Fritsch 1992) in a specified time period
- low-level horizontal moisture convergence
- low-level mass flux at cloud base

with different parameters applied to each of these closures. In the RUC20, a total of 108 closure assumptions are used in the Grell/Devenyi convective scheme. The RUC20 convective scheme also now includes:

- detrainment of cloud water and cloud ice
- entrainment of environmental air into the updraft
- relaxation of stability (convective inhibition) constraints at downstream points based on downdraft strength
- removal of stability constraint at initial time of each model forecast in areas where GOES sounder effective cloud amount (Schreiner et al. 2001) indicates that convection may be present. This technique can aid convection in starting more accurately at grid points where there is positive CAPE, although it cannot create positive CAPE
- correction to exaggerated effects of surface processes in forcing convection. This bug in RUC40 resulted in too widespread convective precipitation over land in summer, especially in the southeastern U.S., and widespread light precipitation over warm ocean areas.



The skill of RUC precipitation forecasts is significantly improved with the RUC20 version, including the Grell/Devenyi ensemble-based convective parameterization. An example of this improvement is presented in Fig. 6, where Figs. 6a,b are 12-h forecasts of 3-h accumulated precipitation from the RUC40 and RUC20 respectively, and Fig. 6c is a radar image in the verifying period. In this case, the RUC20 has accurately forecast much more intensity than the RUC40 to the southern end of a convective line, especially in eastern Louisiana and southern Mississippi. Not only is the intensity improved in the RUC20 forecast, but also the position of the line is more accurately forecast to be farther east than in the RUC40 forecast, stretching from central Ohio into northwestern Alabama before bending back to eastern Louisiana.

Improvement in precipitation forecasts from the RUC20 relative to the RUC40 is also evident in overall precipitation verification statistics over multi-week periods. Daily verification has been performed using the NCEP 24-h precipitation analysis against RUC 24-h totals produced by summing two 12-h forecasts. Two scores traditionally used for precipitation verification, equitable threat score and bias, are used to compare RUC20 and RUC40 forecasts. For a period from spring 2002, the RUC20 has a much higher equitable threat score (Fig. 7a) and bias (Fig. 7b) much closer to 1.0 (preferable) than the RUC40 for almost all precipitation thresholds. Precipitation verification for a November-December 2001 cold season period (Benjamin et al. 2002a) also shows a marked improvement for the RUC20.

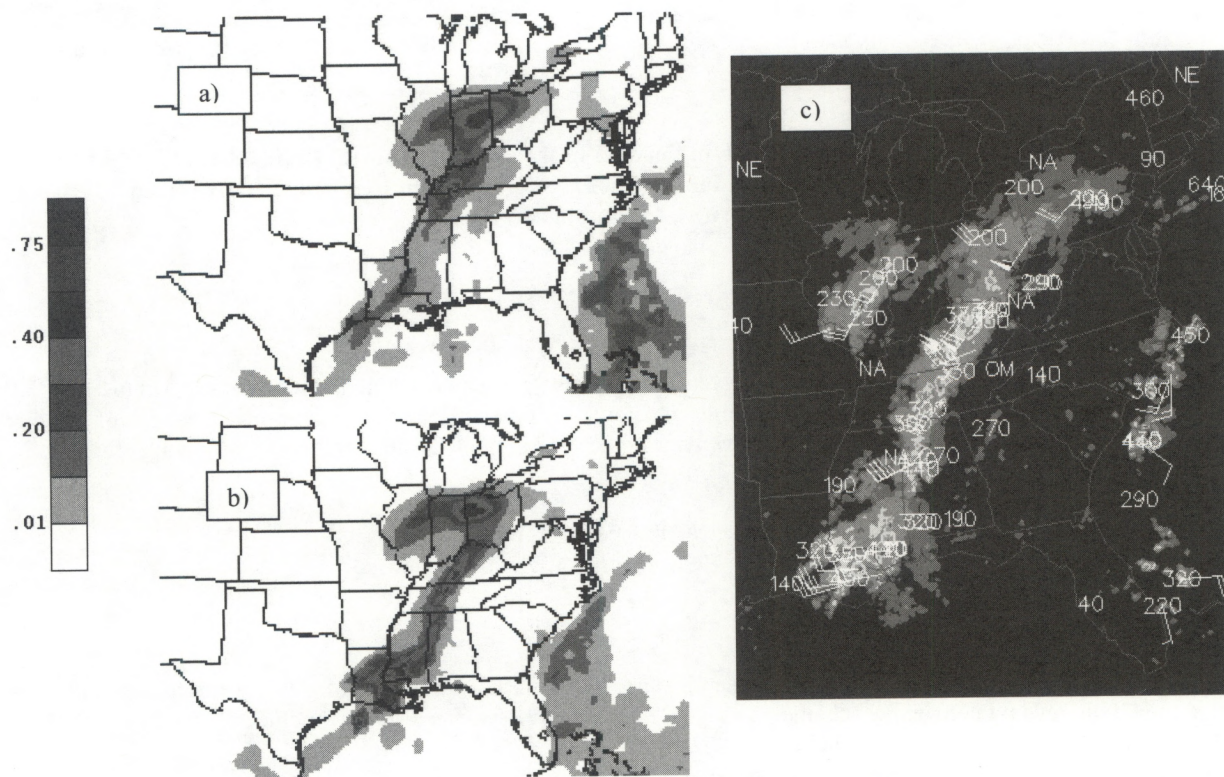


**Figure 6.** Precipitation (in) forecasts initialized at 0000 UTC 26 March 2002 from a) RUC40 and valid at 1115 UTC (verification). RUC20 for 0900–1200 UTC (9–12 h forecasts). c) Radar image in verification period.



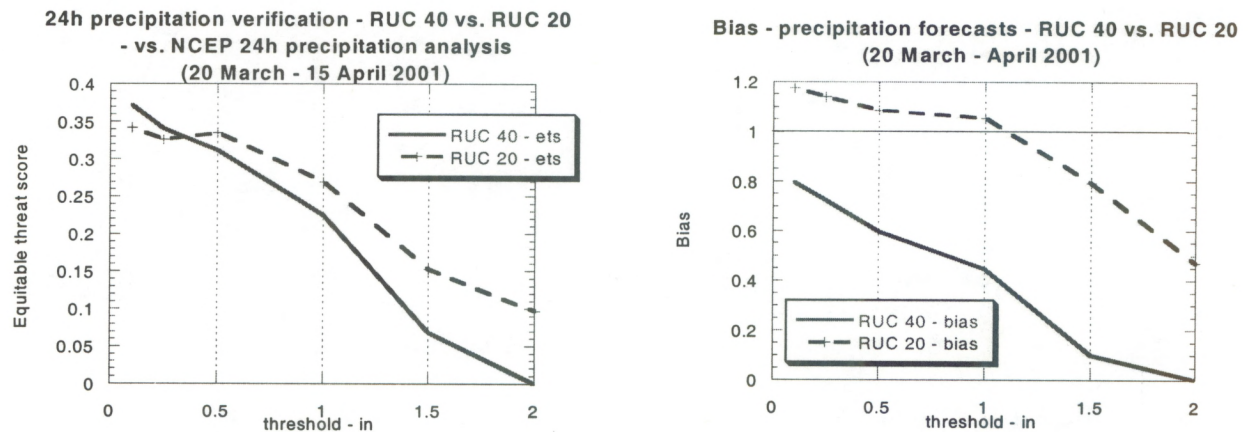


**Figure 7. Precipitation verification comparing RUC20 and RUC40 forecasts, a) (left) equitable threat score and b) bias. Verification is against NCEP 24-h precipitation analysis. For period 20 March–15 April 2001.**

As with the RUC40, the inclusion of downdrafts in the Grell scheme results in smaller-scale details in RUC warm season precipitation patterns than may be evident in that from the Eta model using the Betts-Miller-Janjic convective parameterization. This same difference in character of precipitation forecasts is also evident in NCEP/NSSL experiments comparing the Kain-Fritsch (which also includes downdrafts) and Betts-Miller-Janjic schemes both within the MesoEta model (e.g., Kain et al. 1998).

### 3.2.3 Land-surface physics

A new version of the RUC land-surface model (LSM) is used in the RUC20, including accounting for freezing and thawing of soil, and using a two-layer representation of snow (Smirnova et al. 2000b). This updated LSM is a refinement of the previous RUC40 version discussed in Smirnova et al. (1997). Surface (shelter/anemometer level) forecasts are often critically dependent on accurate estimates of surface fluxes, and in turn, on reasonably accurate soil moisture and temperature estimates. The RUC soil model contains heat and moisture transfer equations solved at 6 levels for each column together with the energy and moisture budget equations for the ground surface. These budgets are applied to a thin layer spanning the ground surface and including both the soil and the atmosphere with corresponding heat capacities and densities. (The budget formulation is one of the primary differences between the RUC LSM and LSMs in other operational models.) A treatment of the evapotranspiration process, developed by Pan and Mahrt (1987), is implemented in the RUC LSM. When snow cover is present, snow is considered to be an additional one or two upper layers of soil, depending on its depth.

To provide a more accurate solution of the energy budget through deeper snow, a snowpack thicker than 7.5 cm is split up into two layers where the top layer is set to be 7.5 cm deep, and the energy budget is applied to the top half of this top layer. A heat budget is also calculated at the boundary between the snow pack and the soil, allowing melting from the bottom of the snow layer. Incorporation of a two-layer snow representation into the land-surface scheme in the RUC20 significantly improves the skin temperatures in winter, and therefore, also the 2-m temperature forecasts (Figs. 8 and 9).

The accumulation of snow on the ground surface is provided by the mixed-phase cloud microphysics algorithm of the RUC forecast scheme (Reisner et al. 1998, Brown et al. 2000, section 3.2.1 of this document). It predicts the total amount of precipitation and also the distribution of precipitation between the solid and liquid phase. In the RUC20, the Grell/Devenyi convective parameterization scheme now also contributes to the snow accumulation if the surface temperature is at or below 0.1°C.



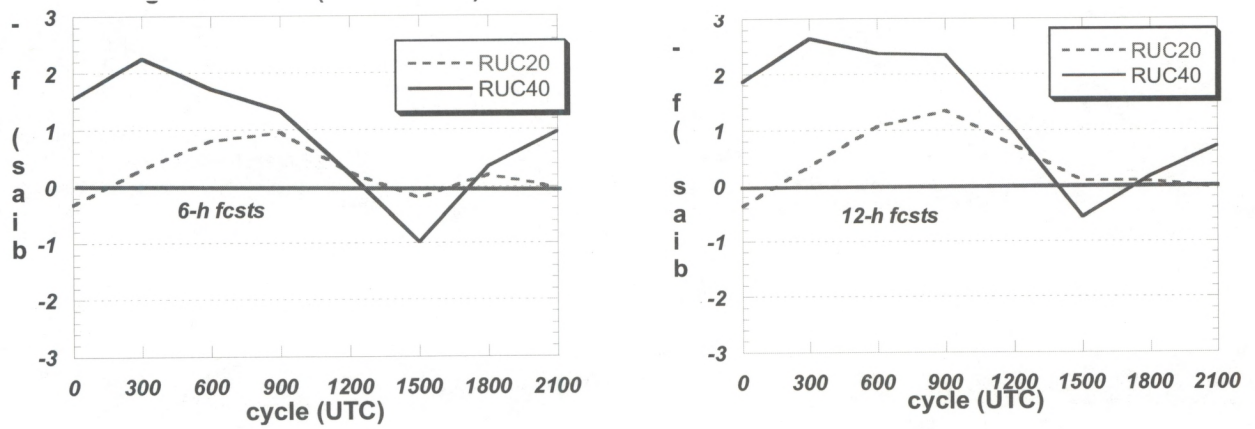


Figure 8. Diurnal variation of 2-m temperature ( $^{\circ}\text{C}$ ) bias (forecast-obs) in RUC20 and RUC40 forecasts. Forecast valid times on horizontal axis. Verification against METAR observations in RUC domain east of  $105^{\circ}\text{W}$ . a) (left) for 6-h forecasts, b) (right) for 12-h forecasts.

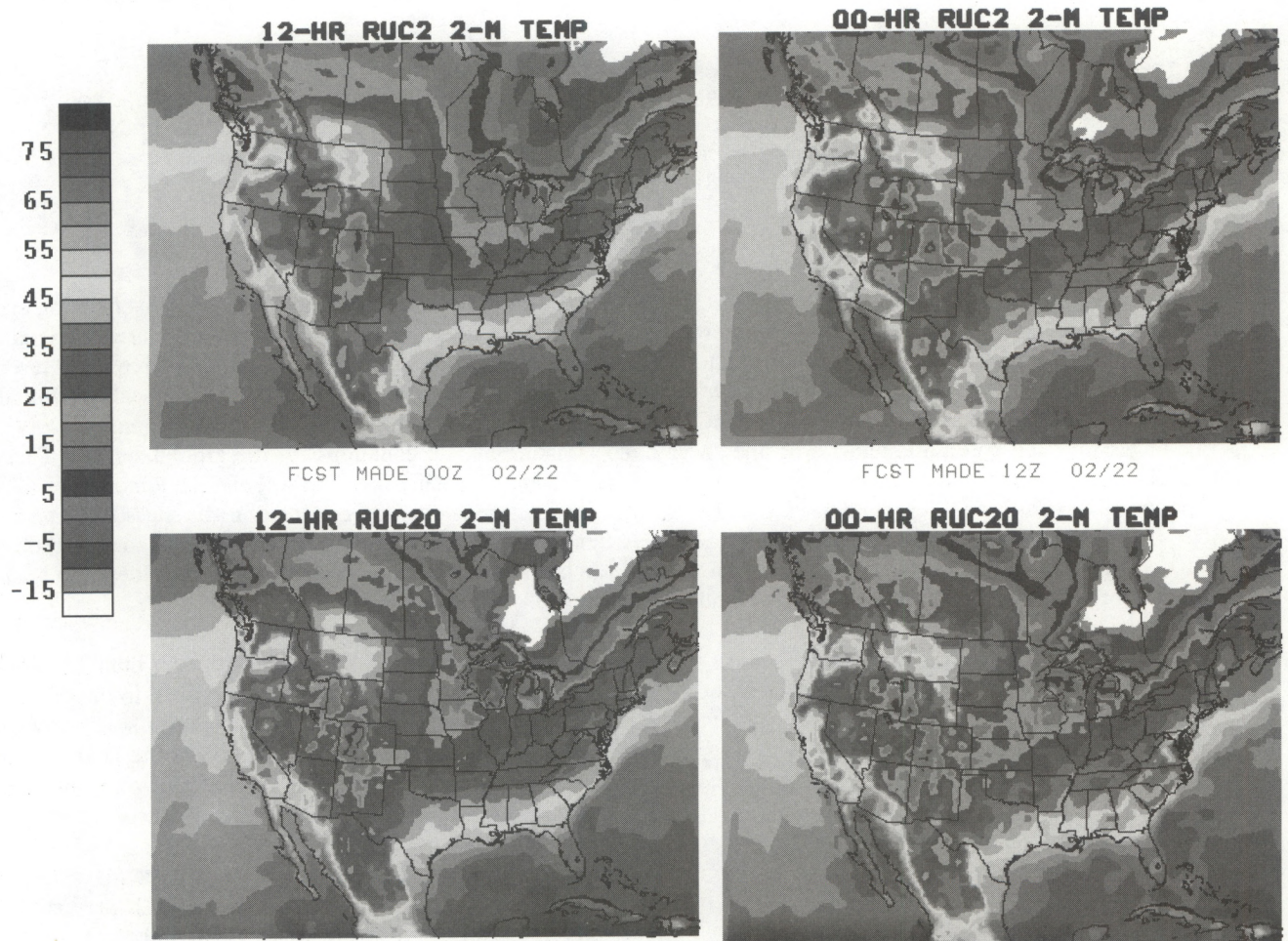


Figure 9. Comparison of 2-m temperature ( $^{\circ}\text{F}$ ) 12-h forecasts from RUC40 (upper left) and RUC20 (lower left) valid 1200 UTC 22 Feb 2002. Verification analyses from RUC40 (upper right) and RUC20 (lower right).



As with the RUC40, the RUC20 cycles volumetric soil moisture and soil temperature at the 6 soil model levels, as well as canopy water, and snow temperature. In the RUC20, cycling of the snow temperature of the second layer (where needed) is also performed. The RUC continues to be unique among operational models in its specification of snow cover and snow water content through cycling (Smirnova et al. 2000b). The two-layer snow model in the RUC20 improves this cycling, especially in spring time, more accurately depicting the snow melting season and spring spike in total runoff, as shown in 1-D experiments with the RUC LSM over an 18-year period from a site in Russia (Smirnova et al. 2000b).

The RUC20 also uses a different formulation for thermal conductivity (Johansen 1975, Peters-Lidard 1998) that generally reduces values of this parameter, especially in near-saturated soils, thereby contributing to a stronger diurnal cycle. This change helps to correct an inadequate diurnal cycle (daytime too cool, nighttime too warm) in the RUC40. Figure 8 shows that the diurnal cycle is better depicted in the RUC20 but that there is still some remaining tendency for inadequate nighttime cooling. An example of improved surface temperature forecasts is provided in Fig. 9, where the RUC20 provides more accurate forecasts in the central plains (cooler), northern Indiana and Ohio (warmer), and central California (cooler) than the RUC40 for this overnight 12-h forecast ending at 1200 UTC 22 Feb 2002. Schwartz and Benjamin (2002) show that the RUC20 provides improved 2-m temperature and 10-m wind forecasts, especially during daytime.

#### **3.2.4 Atmospheric radiation**

The RUC20 continues to use the MM5 atmospheric radiation package (Dudhia 1989, Grell et al. 1994) with additions for attenuation and scattering by all hydrometeor types. This scheme is a broadband scheme with separate components for longwave and shortwave radiation. In the RUC20, the calculation of shortwave radiation is corrected for a 30-min mean time lag in solar radiation present in the RUC40. This correction helps to improve morning near-surface temperature forecasts (e.g., Fig. 8 results for forecasts valid at 1500 UTC). The RUC20 also updates shortwave radiation more frequently, every 30 min instead of every 60 min in RUC40 (Table 4). The updating of longwave radiation remains every 60 min in RUC20, same as RUC40.

#### **3.2.5 Turbulent mixing**

The RUC20 continues to prescribe turbulent mixing at all levels, including the boundary layer, via the explicit turbulence scheme of Burk and Thompson (1989). This scheme is a level-3.0 scheme, with explicit forecast of turbulent kinetic energy and three other turbulence variables. The surface layer mixing continues to be prescribed by Monin-Obukhov similarity theory, specifically the three-layer scheme described in Pan et al. (1994). With the Burk-Thompson scheme, the RUC typically forecasts TKE amounts of 5-20 J/kg in the boundary layer, and also forecasts TKE maxima aloft, typically localized in frontal zones, corresponding to likely areas for clear-air turbulence.

#### **3.2.6 Time splitting for physical parameterizations**

As with other mesoscale models, the RUC gains efficiency by not calling physical parameterizations at the full frequency of each dynamic time step. Time truncation errors are, however, incurred by this time splitting. In the RUC20, the frequency of calls to physical parameterizations has been increased, as is shown in Table 4. Of these changes, the one for the cloud microphysics is most significant, decreasing time truncation errors associated with microphysical processes and precipitation fallout.



**Table 4. Frequency of calls to physical parameterizations in RUC40 and RUC20.**

Physical parameterization	RUC40 frequency (min)	RUC20 frequency (min)
Cloud microphysics	10	2
Convection	5	2
Turbulence	5	2
Land-surface	5	2
Shortwave radiation	60	30
Longwave radiation	60	60

The application of tendencies (rate of change to temperature, moisture, wind, etc.) from the physical parameterizations is also different in RUC20. In RUC40, tendencies from each physics routine except for radiation were applied with the parameterization time step only when the parameterization was called instead of being spread evenly over the interval between calls. This technique, which we inelegantly term “chunking,” causes some shock to the model, although the effects did not seem harmful. In the RUC20, tendencies are applied at each dynamics time step, thus avoiding “chunking.”

#### **4. CHANGES TO LATERAL AND LOWER BOUNDARY CONDITIONS IN RUC20**

##### **4.1 Lateral boundary conditions**

With the RUC20, lateral boundary conditions are specified from Eta model runs made every 6 h. Thus, the lateral boundaries are updated with more recent data than with RUC40, for which new Eta runs were incorporated only every 12 h. The output frequency from the Eta used for the RUC boundary conditions is 3 h. The Eta data used for RUC lateral boundary conditions are currently from 25-hPa 40-km output grids. The Eta model forecasts are interpolated to the RUC20 domain on its hybrid coordinate levels. Values of pressure thickness, virtual potential temperature, and horizontal winds at the edge of the RUC domain (up to 5 grid points from the boundary) are nudged (Davies 1976) toward the Eta values at each time step in a model run. For the RUC20, fixes have been made in application of lateral boundary conditions, resulting in smoother fields near the boundaries.

It is important to note that since the RUC runs prior to the Eta in NCEP’s operational suite, it uses “old” boundary condition data for model forecasts made at 0000 and 1200 UTC. This timing sequence results in a slight degradation of quality of RUC forecasts near the boundaries for runs initialized at these times. Tests at FSL in which the RUC runs at 0000 and 1200 UTC are made *after* Eta boundary conditions are available at those same times show a clear increase in statistical forecast skill.

##### **4.2 Lower boundary conditions**

- Sea-surface temperature – Uses same daily analysis as used for Eta runs (currently, the 50-km global real-time SST analysis from the NCEP/EMC Ocean Modeling Branch). Higher-resolution information for the Great Lakes is also incorporated. The RUC’s use of SST data is set via scripts to follow any changes made for the Eta model.
  - In the RUC20, a bug has been fixed that was causing 1° lat/lon blockiness in the SST used in the RUC40. This blockiness was also apparent in the 2-m temperatures over oceans (e.g., Fig. 10).
  - Monthly climatological values are used for Great Salt Lake in RUC20 but not RUC40 (L. Dunn, personal communication). Time interpolation is to date of month.



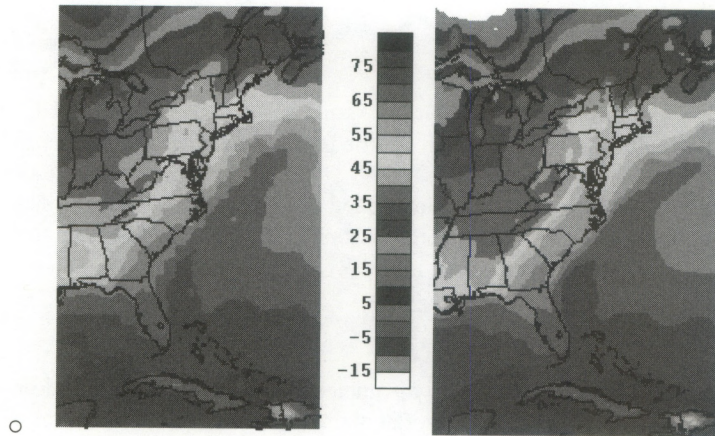


Figure 10. 2-m temperature 12-h forecasts from a) (left) RUC40, b) (right) RUC20, valid at 1200 UTC 21 February 2001.

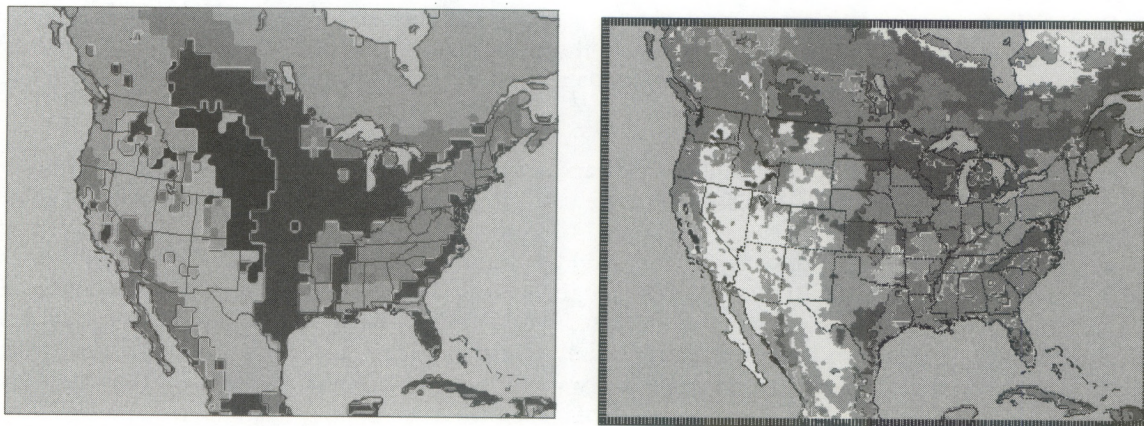


Figure 11. Land-use for a) (left) RUC40 and b) (right) RUC20

- Ice cover — RUC20 uses NESDIS daily ice analysis, same as used by Eta model. No change from RUC40.
- Land use — RUC20 land use (Fig. 11b) is taken from USGS 24-class, 30-second dataset used in MM5 and WRF (Weather Research and Forecasting) model pre-processing programs. RUC40 (Fig. 11a) used old MM4 land-use data with 1° lat/lon resolution and caused blockiness in RUC40 surface fields.
- Soil texture — RUC20 uses much higher resolution information than in RUC40. RUC20 soil type data are taken from a global 30-second dataset, accessible from the WRF preprocessor code.
- Vegetation fraction — For both RUC20 and RUC40, this is specified from monthly high-resolution (0.144°) data produced from 5-year climatology (Gutman and Ignatov 1998) of NDVI (normalized digital vegetation index, an AVHRR-based satellite product). This is the same dataset used by the Eta model. Values are interpolated by date of month between monthly values assumed to be valid on the 15<sup>th</sup> of each month.
- Albedo — For RUC20, this is also specified from NESDIS monthly high-resolution (0.144°) data produced from a 5-year climatology (Csiszar and Gutman 1999), and this is the same dataset used by Eta model. In the RUC40, albedo data were from a much coarser 1° seasonal climatology dataset.
- Terrain elevation — As described in section 2.



## 5. ANALYSIS CHANGES IN RUC20

The RUC20 analysis continues to use an optimal interpolation (OI) analysis applied on the RUC native hybrid isentropic-sigma levels, but with some important modifications from the RUC40 OI analysis, as described below.

[A three-dimensional variational (3DVAR) analysis has been developed for the RUC (Devenyi et al. 2001); some further tuning is needed to squeeze out a little more skill in 3-h forecasts before it can be implemented. It is hoped that the RUC 3DVAR can be implemented 5–6 months after the initial RUC20 implementation.]

### 5.1 Assimilation of GOES cloud-top pressure data

Toward the goal of improved short-range forecasts of cloud/hydrometeors, icing, and precipitation, an advanced version of the RUC cloud-top pressure assimilation technique (Benjamin et al. 2002b) has been developed and tested. This improved technique, using GOES single field-of-view cloud-top pressure and temperature data provided by NESDIS, is being implemented into operations with the rest of the RUC20. As described in section 3.2.1, the RUC uses a bulk mixed-phase cloud microphysics scheme from the NCAR/Penn State MM5 model, with five hydrometeor types explicitly forecast (Brown et al. 2000). The prognostic variables in this scheme are mixing ratios of water vapor, cloud water, rainwater, ice, snow, and graupel, and number concentration of ice particles. In the RUC40, the initial conditions for the fields were simply those carried over from the previous 1-h RUC forecast. In the RUC20 including assimilation of GOES cloud-top data, these fields are modified each hour as part of the cloud clearing and cloud building.

The RUC20 cloud/hydrometeor analysis technique is an advanced version of the procedures previously described by Kim and Benjamin (2001, 2000). GOES cloud-top pressure data provide information on the horizontal location of cloudy and cloud-free areas, but not on cloud depth. Also, unless there are broken layers, it cannot provide information on multiple cloud layers. Thus, the RUC cloud/hydrometeor assimilation technique is designed to use this partial information. When GOES data indicate that no clouds are present, the technique removes any hydrometeors and reduces water vapor mixing ratio to a subsaturation value. When GOES data indicate that cloud not present in the RUC 1-h forecast at the correct level, cloud water and/or ice is added in a layer of not more than 50 hPa depth. This layer is also saturated with respect to water or ice with a linear variation between these two saturation vapor pressure values in the 248–263 K range.

Other features of the RUC GOES cloud-top assimilation include:

- Rederivation of cloud-top pressure from GOES cloud-top temperature if the original retrieval of cloud-top pressure is closer to the ground than 620 hPa. This rederivation of the cloud-top pressure uses the RUC 1-h temperature/moisture profile at the nearest grid point.
- Use of single field-of-view GOES data (~10-km resolution). The median values from the fields-of-view around each RUC box are used. With this sampling, cloud fraction is calculated in RUC grid volumes.
- Use of stability check to identify possible sub-field-of-view variations from small convective clouds that result in inaccurate cloud-top temperature and pressure determination.
- Remove cloud indicators if they only occur at isolated (noncontiguous) RUC grid points, again on the presumption that GOES may be observing sub-field-of-view clouds.
- Special handling for marine stratus situations to force cloud-top at consistent level with top of marine inversion in RUC background profile.
- Information from the GOES effective cloud amount is used to modify a stability constraint for convection in the subsequent forecast run (see section 3.2.2).



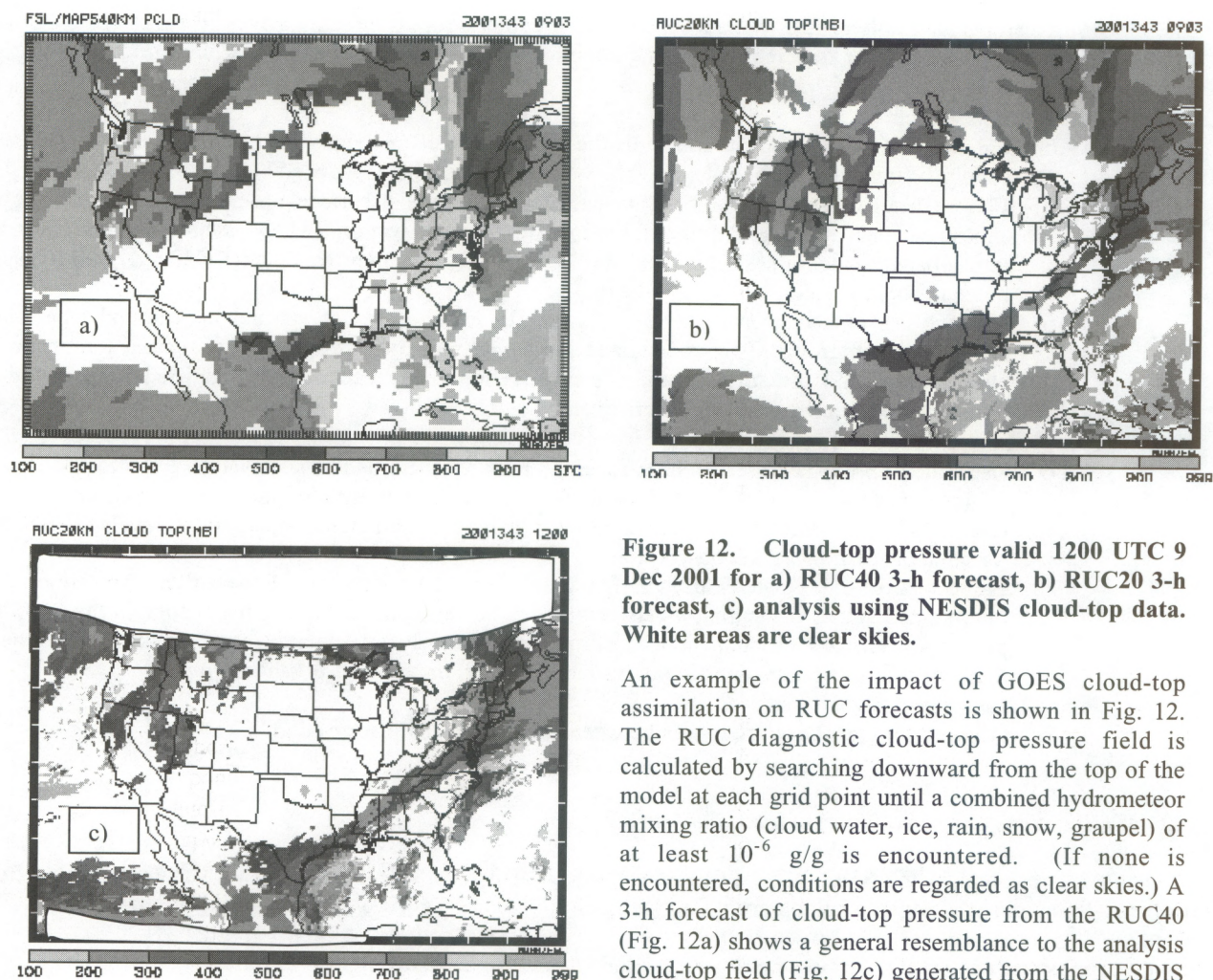


**Figure 12.** Cloud-top pressure valid 1200 UTC 9 Dec 2001 for a) RUC40 3-h forecast, b) RUC20 3-h forecast, c) analysis using NESDIS cloud-top data. White areas are clear skies.

An example of the impact of GOES cloud-top assimilation on RUC forecasts is shown in Fig. 12. The RUC diagnostic cloud-top pressure field is calculated by searching downward from the top of the model at each grid point until a combined hydrometeor mixing ratio (cloud water, ice, rain, snow, graupel) of at least  $10^{-6}$  g/g is encountered. (If none is encountered, conditions are regarded as clear skies.) A 3-h forecast of cloud-top pressure from the RUC40 (Fig. 12a) shows a general resemblance to the analysis cloud-top field (Fig. 12c) generated from the NESDIS cloud product, but the RUC20 3-h forecast (Fig. 12b) shows much better agreement with the analysis. This improved forecast is due not only to the cloud-top assimilation (and retention in the subsequent forecast), but also to other changes in the RUC20 including improved microphysics and higher resolution.

Ongoing statistical verification has been performed, calculating correlation coefficients between the NESDIS cloud-top product and RUC40 and RUC20 forecasts of durations from 1 h to 12 h. These statistics (Benjamin et al. 2002b) show that the RUC20 produces improved cloud-top forecasts over RUC40 not just at 1-h and 3-h projections, but with similar improvement out to 12-h forecasts.

## 5.2 Improved observation preprocessing

The most important changes in the RUC20 OI analysis are the observation preprocessing and matching to background values. In the observation preprocessing, a more flexible, lower-memory, observation array structure is used in the RUC20 that allows each level of a profile observation (e.g., rawinsonde, profiler, VAD) to be associated with its own metadata (position, time, expected error) if necessary. This structure was developed for the RUC 3DVAR but is also used in the RUC20 OI analysis. It allows, among other things, for use of varying positions to account for balloon drift in rawinsonde observations. However, the decision was made to not incorporate balloon drift in the RUC20 analysis since the effects of time change and position drift largely cancel each other.



The following features are implemented in the RUC20 observation preprocessing to improve the use of observations in the analysis. The goal of these features is to match the information in the observation and background as nearly as possible.

- Surface observations
  - Calculate 2-m temperature and moisture values and 10-m winds from background, instead of simply taking the 5-m background values. The result of this is reduced bias in the analysis.
  - Choose nearest land grid point from background for most surface observations over land, but choose nearest water grid point for buoy surface observations when calculating observation-minus-background values for coastal surface stations. This improves the RUC20 analyzed surface fields in coastal regions.
  - Improve use of background model lapse rate to match observations and background when the elevation is different. This constrained lapse rate reduction is applied for surface temperature observations, and the surface moisture observation is correspondingly modified such that the original dewpoint depression is maintained.
- Rawinsonde/profiler observations
  - Use code to preserve observed near-surface structure when rawinsonde surface elevation does not match that of model background. This logic is similar to that used for surface observations.
  - Use raw level observations now in addition to values interpolated to background levels (also used for wind profiler and VAD observations).
  - Prevent use of interpolated values if significant level data not present. For profilers, prevent use of interpolated values if separation between raw values exceeds 1200 m. This change in the RUC20 prevents a RUC40 problem in which unrealistic linearly interpolated profiles were used when there were large vertical gaps in rawinsonde, profiler, or VAD observation profiles.
- Precipitable water observations
  - Account for elevation differences between observation and background.

### 5.3 Modifications to optimal interpolation analysis

A detailed description of the RUC OI analysis from the RUC40 is available in the RUC-2 Technical Procedures Bulletin (Benjamin et al. 1998, available from the NWS at <http://205.156.54.206/om/tpb/448.htm> ).

Modifications made in the RUC20 to other aspects of the OI analysis are listed below.

- Quality control – Continues to use the OI-based buddy check. In RUC20, a buddy check is now performed for cloud-drift winds and precipitable water observations (not in RUC40) and bugs are fixed. RUC20 honors NCEP observation QC flags, which was not done in RUC40. This means, for instance, that quality flags from the NOAA Profiler Hub are now being used.
- Improved observation search strategy allowing much more complete use of aircraft ascent/descent profiles than in RUC40.
- Moisture analysis looping – In order to force some interconsistency in the RUC20 analysis between different moisture observations, a two-pass loop is performed. Within each loop, the analysis order is as follows: cloud-top observations, precipitable water observations, in situ moisture observations. The observation-minus-background values are recalculated after each part of the moisture analysis, and in situ observations are given the “last say.”
- Moisture variable – changed from condensation pressure in RUC40 to natural logarithm of water vapor mixing ratio ( $\ln q$ ). This simplifies the variable transformation needed for precipitable water analysis and cloud-top assimilation. The variable  $\ln q$  is conserved under motion in adiabatic conditions, considered to be desirable for the choice of an analysis variable. The cycled water vapor variable in the RUC and prognostic variable in the RUC model continues to be water vapor mixing ratio.
- Constraints applied at end of analysis
  - A series of top-down and bottom-up lapse rate checks are applied which are designed to prevent unrealistic lapse rates from occurring in the RUC20 temperature profiles. These checks also improve the retention of surface temperature observations under conditions of a deep boundary layer. A shallow superadiabatic layer near the surface of up to 1.5 K is allowed in these checks.



- Supersaturation is removed (also performed in RUC40 analysis).
- NCEP quality control flags for individual observations are used, and suspect observations are flagged so that they will not be used in the RUC20 analysis.
- More robust hybrid coordinate adjustment.

The RUC20 OI analysis has been tested extensively at FSL with three additional new observation types:

- GPS ground-based precipitable water values (now over 100 in U.S.)
- 915 MHz boundary-layer profilers (about 25 in RUC domain)
- RASS temperature low-level virtual temperature profiles from selected 405 MHz and 915 MHz profilers

Work by FSL and NCEP is nearly complete to make these observations available to the RUC and other NCEP operational models, and it is likely that they will be added to the RUC20 within three months after its initial implementation.

## 6. RUC20 OUTPUT FILES AND VARIABLES

### 6.1 Output files

The output files from the RUC20 are essentially the same as those produced by the RUC40, except that they will be available at both 20-km and 40-km resolution. The 40-km files are meant to provide “look-alike” files so that the change will be relatively transparent to RUC users. A list of the variables in each of these files is provided at <http://ruc.fsl.noaa.gov/ruc2vars.html>. The gridded files provided by the RUC20 are reviewed below:

- Native (bgrb, bgrb20) files – 14 3-D variables (no change from RUC40) and 46 2-D variables (the last 8 are new, but the first 38 are identical to those being produced currently by the RUC40).
  - There are 50 vertical levels in the bgrb files at both 20-km and 40-km resolution, different from the 40 levels in the RUC40 bgrb files.
- Isobaric (pgrb, pgrb20) files – 6 3-D variables at 25-hPa vertical resolution from 1000–100 hPa and 88 2-D variables (surface, precipitation, mean-layer values, etc.). Surface pressure substituted for altimeter setting. Otherwise, no change from RUC40 variables.
- Surface (sgrb, sgrb20) files – 25 2-D variables (surface, precipitation, precipitation type, stability indices, etc.). Surface pressure substituted for altimeter setting. Otherwise, no change from RUC40 variables. All fields in the sgrb files are also found in the pgrb files.

Improved BUFR data are available from RUC20. Hourly BUFR soundings with the same format as used for the Eta model are available with the RUC20, including individual station files. These individual station files (only ~25-50 KB each) were not available with the RUC40. The hourly output to 12 h is also new with the RUC20. The station list is the same as that used for the Eta model for stations within the RUC domain. (One small difference in the BUFR data is that the RUC uses 6 soil levels compared with four levels with Eta BUFR output.) The so-called “monolithic” files with all stations and all output times are also available from the RUC20.

A summary of this information is available at <http://ruc.fsl.noaa.gov/ruc20.data-access.html>.

### 6.2 Changes to GRIB identifiers for RUC20

When the RUC40 was implemented, some GRIB parameter values were used on an interim basis until official designations were made. Since the RUC40 implementation, these GRIB parameter values have been officially assigned. These updated parameter values have also been changed (see Table 5) in the RUC20.



**Table 5. Changes in GRIB variable parameters in RUC20**

Field	Parameter value in RUC40	Parameter value in RUC20
Water vapor mixing ratio	185	53
Gust wind speed	255	180
Soil moisture availability	199	207
Soil volumetric moisture content	86	144

Also, the GRIB level parameter for snow temperature is corrected from 116 in RUC40 to 111 in RUC20.

### 6.3 Basic 3-D output variables

There is no change in the 3-D variables output by the RUC20 for either bgrb (native) or pgrb (isobaric) fields resulting from postprocessing changes except that isobaric heights from the RUC20 are smoother due to extra smoothing passes.

### 6.4 RUC 2-D diagnosed variables

As with the 3-D fields, the 2-D fields from the RUC20 are different from those produced by the RUC40 due to all of the analysis, model, resolution, etc. changes listed in previous sections. Below are listed 2-D output variables for which there are significant changes from changes in diagnostic techniques or for other reasons not previously addressed in this document.

- *2-m temperature and dewpoint, and 10-m winds* – Similarity theory is used to derive values at these levels rather than the previous approximation of simply using the 5-m values. Note that the RUC20 continues to use a separate topography file (TOPOMINI, recalculated for 20km resolution) designed to more closely match METAR elevations than the model elevation, as shown in Table 6. The 20-km TOPOMINI matches the METAR elevations more closely than the 40-km version. The 2-m temperature and dewpoint temperature values from the RUC are *not* from the model terrain but are instead reduced to the TOPOMINI elevation. Thus, the RUC20 2-m temperature and dewpoint values include effects both from reduction to the TOPOMINI elevation and similarity reduction to 2 m above the surface. In the RUC20, the TOPOMINI is based not only on the minimum 10-km values within each 20-km grid box, but also includes a subsequent correction from METAR station elevations using a very short-length Cressman analysis.
- *Convective available potential energy* – Some bug fixes resulting in smoother CAPE and CIN (convective inhibition) fields.
- *Helicity* – Corrections to helicity and storm-relative motion calculations, including change to Bunkers et al. (2000) formulation.
- *MAPS mean sea-level pressure* – Bug fixed for reduction over higher terrain, resulting in more coherent SLP patterns than in RUC40.
- *Precipitation type* – Less diagnosis of sleet (ice pellets) in RUC20 due to cloud microphysics changes described in section 3.2.1.
- *Visibility* (see Smith et al. 2002, Smirnova et al. 2000a) – RUC20 diagnostic changed to use multiple levels near surface for hydrometeor and relative humidity and modification in hydrometeor and relative humidity effects. An example of an improved visibility diagnostic is shown in Fig. 13, a situation with widespread fog in the southeastern U.S.



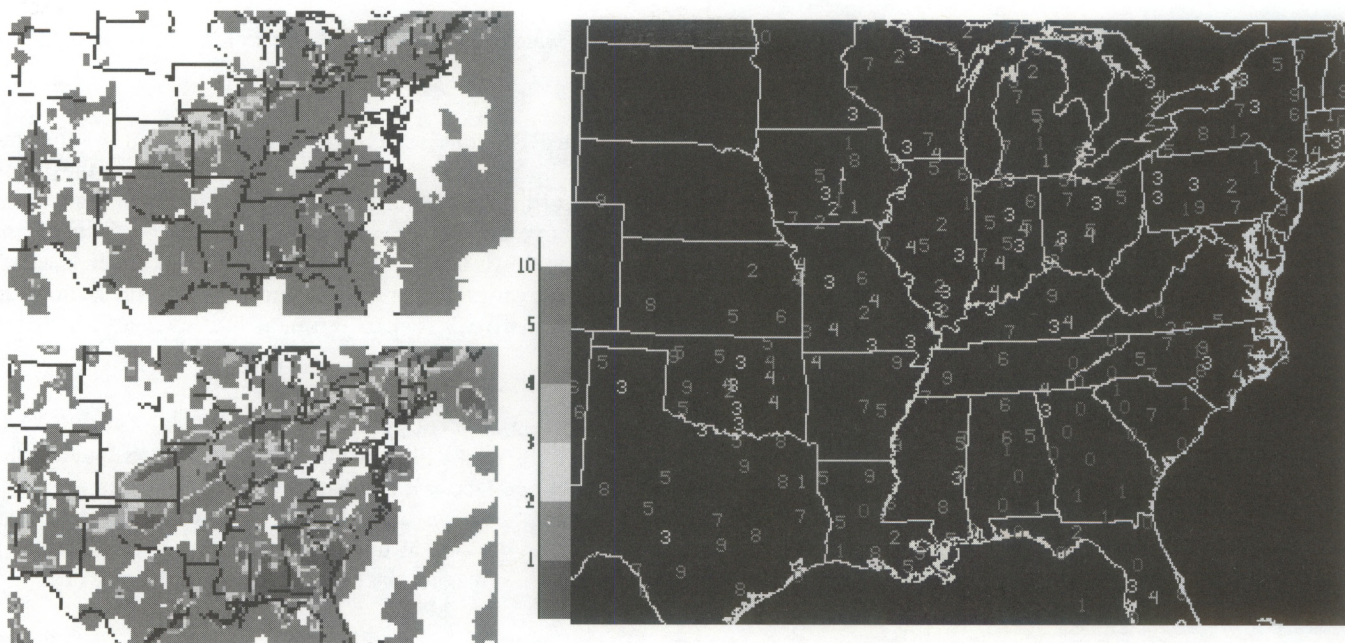


Figure 13. Visibility (mi) valid at 1200 UTC 30 January 2002. a) (upper left) RUC40 0-h forecast, b) (lower left) RUC20 0-h forecast, c) (right) METAR observations.

Table 6. Terrain elevation difference between station elevation and interpolated RUC20 elevation for selected rawinsonde stations in western United States. Column 2 shows this difference for the RUC20 model elevation field, and column 3 shows this difference for the RUC20 TOPOMINI elevation used for reducing 2-m temperature and dewpoint fields.

Rawinsonde station	Station elevation minus RUC20 model elevation (m)	Station elevation minus RUC20 TOPOMINI elevation (m)
Edwards AFB, CA	41	-20
Denver, CO	26	28
Grand Junction, CO	323	6
Boise, ID	253	69
Great Falls, MT	29	-29
Reno, NV	144	-83
Elko, NV	152	-27
Medford, OR	346	105
Salem, OR	51	6
Rapid City, SD	45	-70
Salt Lake City, UT	438	10
Riverton, WY	119	-74

A detailed description of techniques to derive RUC diagnostic variables is available at <http://ruc.fsl.noaa.gov/vartxt.html>. Some of these are listed below, and are unchanged from RUC40.



**Relative humidity** – Defined with respect to saturation over water in the RUC isobaric fields and in the surface relative humidity field.

**Freezing levels** – Two sets of freezing levels are output from RUC, one searching from the bottom up, and one searching from the top down. Of course, these two sets will be equivalent under most situations, but they may sometimes identify multiple freezing levels. The bottom-up algorithm will return the surface as the freezing level if any of the bottom three native RUC levels (up to about 50 m above the surface) are below freezing (per instructions from Aviation Weather Center, which uses this product). The top-down freezing level returns the first level at which the temperature goes above freezing searching from the top downward. For both the top-down and bottom-up algorithms, the freezing level is actually interpolated between native levels to estimate the level at which the temperature goes above or below freezing.

**Tropopause pressure** – Diagnosed from the 2.0 isentropic potential vorticity unit (PVU) surface. The 2.0 PVU surface is calculated directly from the native isentropic/sigma RUC grids. First, a 3-D PV field is calculated in the layers between RUC levels from the native grid. Then, the PV=2 surface is calculated by interpolating in the layer where PV is first found to be less than 2.0 searching from the top down in each grid column. Low tropopause regions correspond to upper-level waves and give a quasi-3D way to look at upper-level potential vorticity. They also correspond very well to dry (warm) areas in water vapor satellite images, since stratospheric air is very dry.

**MAPS mean sea-level pressure** – This reduction (Benjamin and Miller 1990) is the one used in previous versions of the RUC. It uses the 700 hPa temperature to minimize unrepresentative local variations caused by local surface temperature variations. It has some improvement over the standard reduction method in mountainous areas and gives geostrophic winds that are more consistent with observed surface winds. As noted earlier, a bug fix for reduction over higher terrain is included in the RUC20, improving the coherence of the sea-level pressure pattern in these areas.

**3-h surface pressure change** – These fields are determined by differencing surface pressure fields at valid times separated by 3 h. Since altimeter setting values (surface pressure) are used in the RUC analyses, this field reflects the observed 3-h pressure change fairly closely over areas with surface observations. It is based on the forecast in data-void regions. The 3-h pressure change field during the first 3 h of a model forecast often shows some non-physical features, resulting from gravity wave sloshing in the model. After 3 h, the pressure change field appears to be quite well-behaved. The smaller-scale features in this field appear to be very useful for seeing predicted movement of lows, surges, etc. despite the slosh at the beginning of the forecast.

**2-m temperature, dewpoint temperature** – Temperature and dewpoint temperatures displayed are extrapolated to a "minimum" topography field to give values more representative of valley stations in mountainous areas, where surface stations are usually located.

**Precipitation accumulation** – All precipitation values, including the 12-h total, are liquid equivalents, regardless of whether the precipitation is rain, snow, or graupel.

**Resolvable and subgrid-scale precipitation** – The Grell family of convective schemes used in the RUC tends to force grid-scale saturation in its feedback to temperature and moisture fields. One result of this is that for the RUC model, some of the precipitation from weather systems that might be considered to be largely convective will be reflected in the resolvable-scale precipitation. Thus, the subgrid-scale precipitation from RUC should *not* be considered equivalent to "convective precipitation."

**Snow accumulation** – Snow accumulations are calculated using a 10 to 1 ratio between snow and liquid water equivalent. Of course, in reality, the ratio of snow to liquid water equivalent varies, but the ratio used here was set at this constant value so that users will know the water equivalent exactly.



Also, snow accumulation (through the snow liquid water equivalent) is not diagnosed based on temperature, but is explicitly forecast through the mixed-phase cloud microphysics in the RUC model.

**Categorical precipitation types (rain/snow/ice pellets/freezing rain)** – These yes/no indicators are calculated from the explicit cloud microphysics in the RUC model (see section 3.2.1). *These values are not mutually exclusive. More than one value can be yes (1) at a grid point. In other words, the RUC can predict mixed precipitation types.* Here is how the diagnostics are done:

Diagnostic logic for precipitation types

- Snow
  - There are a few ways to get snow.
  - If fall rate for snow mixing ratio at ground is at least  $0.2 \times 10^{-9}$  g/g/second, snow is diagnosed.
  - If fall rate for graupel mixing ratio at ground is  $> 1.0 \times 10^{-9}$  g/g/s and
    - surface temp is  $< 0$  deg C, and max rain mixing ratio at any level  $< 0.05$  g/kg or the graupel rate at the surface is less than the snow fall rate, snow is diagnosed.
    - surface temp is between  $0 - +2$  deg C, snow is diagnosed.
- Rain – If the fall rate for rain mixing ratio at ground is at least  $0.01$  g/g/second, and the temperature at the surface is  $> \text{or} = 0$  deg C, then rain is diagnosed. The temperature used for this diagnosis is that at the minimum topography, described above.
- Freezing rain – Same as for rain, but if the temperature at the surface is  $< 0$  deg C **and** some level above the surface is above freezing, freezing rain is diagnosed.
- Ice pellets – If
  - the graupel fall rate at the surface is at least  $1.0 \times 10^{-9}$  g/g/s and
  - the surface temp is  $< 0$  deg C and the max rain mixing ratio in the column is  $> 0.05$  g/kg and
  - the graupel fall rate at the surface is greater than that for snow mixing ratio,then ice pellets are diagnosed.

**CAPE** (Convective available potential energy) – Energy available for buoyant parcel from native RUC levels with maximum buoyancy within 300 hPa of surface. Before the most buoyant level is determined, an averaging of potential temperature and water vapor mixing ratio is done in the lowest seven RUC native levels (about 40 hPa).

**CIN** (Convective inhibition) – Negative buoyant energy in layer through which a potentially buoyant parcel must be lifted before becoming positively buoyant.

**Lifted index / Best lifted index** – Lifted index uses the surface parcel, and best lifted index uses buoyant parcel from the native RUC level with maximum buoyancy within 300 hPa.

**Precipitable water** – Integrated precipitable water vapor from surface of RUC model to top level (~50 hPa). The precipitable water calculation is performed by summing the product of the specific humidity at each level times the mass of each surrounding layer. This mass layer is bounded by the midpoints between each level, since the native RUC vertical grid is nonstaggered.

## 7. STATISTICAL VERIFICATION AGAINST RAWINSONDES

RUC20 forecast skill was compared with that of the RUC40 for retrospective periods from February 2001 (cold season, statistics at <http://www.emc.ncep.noaa.gov/mmb/ruc2/oiretrostats/>) and July 2001 (warm season, statistics at <http://www.emc.ncep.noaa.gov/mmb/ruc2/summerretrostats/>). In addition, recent real-time runs provide results from cold season and transition season periods (statistics at <http://www.emc.ncep.noaa.gov/mmb/ruc2/stats/>). In general, RUC20 analyses do not fit rawinsonde data quite as closely at this time as RUC40 analyses. This may be due to improved use of aircraft ascent/descent data in the case of wind and temperature analyses, and the use of  $\ln q$  as a moisture analysis variable in the case of relative humidity.



For wind forecasts (Fig. 14a), the RUC20 provides some improvement over the RUC40 for 3-h forecasts (margin 0–0.3  $\text{ms}^{-1}$ ) and for 12-h forecasts (margin 0.1–0.4  $\text{m s}^{-1}$ ). For temperatures (Fig. 14b), the RUC20 again gives some improvement by this measure, especially in the lower troposphere.

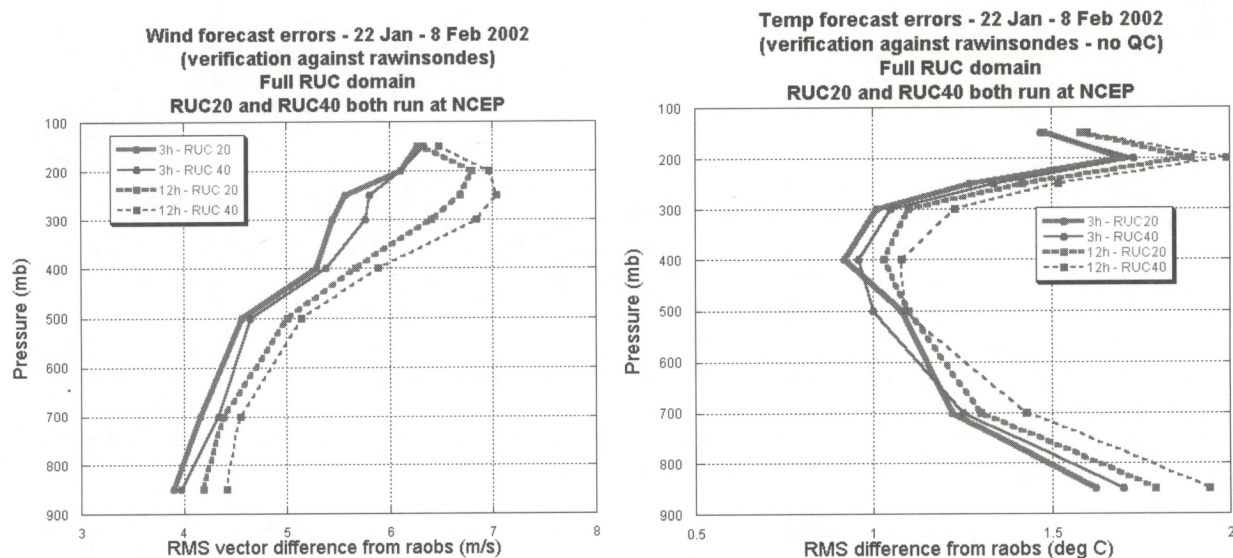


**Figure 14. Verification of RUC40 and RUC20 3-h and 12-h forecasts against rawinsonde observations. For a) (left) wind, and b) (right) temperature, and for period 22 January – 8 February 2002.**



## 8. REFERENCES

RUC web page – <http://ruc.fsl.noaa.gov> – real time products and a great deal of other information including a more complete list of references

- Arakawa, A., and V.R. Lamb, 1977: Computational design of the basic dynamical processes of the UCLA general circulation model. *Methods in Computational Physics*, Vol. 17, Academic Press, 174-265, 337 pp.
- Benjamin, S.G., J.M. Brown, D. Devenyi, G.A. Grell, D. Kim, T.L. Smith, T.G. Smirnova, B.E. Schwartz, S. Weygandt, K.J. Brundage, and G.S. Manikin, 2002a: The 20-km Rapid Update Cycle--Overview and implications for aviation applications. *10th Conf. on Aviation, Range, and Aerospace Meteorology*, Portland, OR, Amer. Meteor. Soc., 24-27. (available in PDF from <http://ruc.fsl.noaa.gov> under 'RUC pubs')
- Benjamin, S.G., D. Kim, and J.M. Brown, 2002b: Cloud/hydrometeor initialization in the 20-km RUC with GOES and radar data. *10th Conf. on Aviation, Range, and Aerospace Meteorology*, Portland, OR, Amer. Meteor. Soc., 232-235. (available in PDF from <http://ruc.fsl.noaa.gov> under 'RUC pubs')
- Benjamin, S.G., J.M. Brown, K.J. Brundage, B.E. Schwartz, T.G. Smirnova, T.L. Smith, L.L. Morone, 1998: RUC-2 - The Rapid Update Cycle Version 2. NWS Technical Procedure Bulletin No. 448. NOAA/NWS, 18 pp. [National Weather Service, Office of Meteorology, 1325 East-West Highway, Silver Spring, MD 20910] Available online at <http://205.156.54.206/om/tpb/448.htm> ).
- Benjamin, S.G., K.J. Brundage, and L.L. Morone, 1994: The Rapid Update Cycle. Part I: Analysis/model description. Technical Procedures Bulletin No. 416, NOAA/NWS, 16 pp. [National Weather Service, Office of Meteorology, 1325 East-West Highway, Silver Spring, MD 20910].
- Benjamin, S. G., K. A. Brewster, R. L. Brummer, B. F. Jewett, T. W. Schlatter, T. L. Smith, and P. A. Stamus, 1991: An isentropic three-hourly data assimilation system using ACARS aircraft observations. *Mon. Wea. Rev.*, **119**, 888-906.
- Benjamin, S. G., and P. A. Miller, 1990: An alternative sea-level pressure reduction and a statistical comparison of surface geostrophic wind estimates with observed winds. *Mon. Wea. Rev.*, **118**, 2099-2116.
- Benjamin, S. G., 1989: An isentropic meso-alpha scale analysis system and its sensitivity to aircraft and surface observations. *Mon. Wea. Rev.*, **117**, 1586-1603.
- Bleck, R., and S.G. Benjamin, 1993. Regional weather prediction with a model combining terrain-following and isentropic coordinates. Part I: model description. *Mon. Wea. Rev.*, **121**, 1770-1885.
- Brown, J.M., T.G. Smirnova, S.G. Benjamin, R. Rasmussen, G. Thompson, and K. Manning, 2000: Use of a mixed-phase microphysics scheme in the operational NCEP Rapid Update Cycle. *9th Conf. on Aviation, Range, and Aerospace Meteorology*, Amer. Meteor. Soc., Orlando, FL, 100-101.
- Bunkers, M.J., B.A. Klimowski, J.W. Zeitler, R.L. Thompson, M.L. Weisman, 2000: Prediction of supercell motion using a new hodograph technique. *Wea. Forecast.*, **15**, 61-79.
- Burk, S.D., and W.T. Thompson, 1989: A vertically nested regional numerical prediction model with second-order closure physics. *Mon. Wea. Rev.*, **117**, 2305-2324.
- Csiszar, I. and G. Gutman, 1999: Mapping global land surface albedo from NOAA/AVHRR. *J Geophys. Res.* **104**, 6215-6228.
- Davies, H.C., 1976: A lateral boundary formulation for multi-level prediction models. *Tellus*, **102**, 405-418.
- Devenyi, D., S.G. Benjamin, and S.S. Weygandt, 2001: 3DVAR analysis in the Rapid Update Cycle. *14th Conf. on Numerical Weather Prediction*, Fort Lauderdale, FL, Amer. Meteor. Soc., J103-J107.
- Dudhia, J., 1989: Numerical study of convection observed during the winter monsoon experiment using a mesoscale two-dimensional model. *J. Atmos. Sci.*, **46**, 3077-3107.
- Govett, M.W., D.S. Schaffer, T.Henderson, L.B. Hart, J.P. Edwards, C.S. Lior and T.L. Lee, 2001: SMS: A directive-based parallelization approach for shared and distributed memory high performance computers. Proceedings 9<sup>th</sup> ECMWF Workshop on the Use of High Performance Computing in Meteorology, Volume: Developments in TeraComputing, *World Scientific*, 251-268.
- Grell, G.A., 1993: Prognostic evaluation of assumptions used by cumulus parameterizations. *Mon. Wea. Rev.*, **121**, 764-787.
- Grell, G.A., J. Dudhia, and D.R. Stauffer, 1994: A description of the fifth-generation Penn State/NCAR Mesoscale Model (MM5). NCAR Technical Note, NCAR/TN-398 + STR, 138 pp.



- Grell, G.A., and D. Devenyi, 2001: Parameterized convection with ensemble closure/feedback assumptions. *9th Conf. on Mesoscale Processes*, Fort Lauderdale, FL, Amer. Meteor. Soc., 12-16.
- Gutman, G. and A. Ignatov, 1998: The derivation of green vegetation fraction from NOAA/AVHRR for use in numerical weather prediction models. *Int. J. Remote Sens.*, **19**, 1533-1543.
- Johansen, O., 1975: Thermal conductivity in soils. Ph.D. thesis, University of Trondheim, 236 pp. (English translation 637, Cold Reg. Res. and Eng. Lab., Hanover, N.H., 1977).
- Johnson, D.R., T.H. Zapotocny, F.M. Reames, B.J. Wolf, and R.B. Pierce, 1993: A comparison of simulated precipitation by hybrid isentropic-sigma and sigma models. *Mon. Wea. Rev.*, **121**, 2088-2114.
- Johnson, D.R., A.J. Lenzen, T.H. Zapotocny, and T.K. Schaack, 2000: Numerical uncertainties in the simulation of reversible isentropic processes and entropy conservation. *J. Climate*, **13**, 3860-3884.
- Kain, J.S., and J.M. Fritsch, 1992: The role of the convective "trigger function" in numerical forecasts of mesoscale convective systems. *Meteor. Atmos. Phys.*, **49**, 93-106.
- Kain, J.S., M.E. Baldwin, D.J. Stensrud, T.L. Black, and G.S. Manikin, 1998: Considerations for the implementation of a convective parameterization in an operational mesoscale model. *12th Conf. Num Wea. Pred.*, Amer. Meteor. Soc., Phoenix, 103-106.
- Kim, D., and S.G. Benjamin, 2001: Cloud/hydrometeor initialization for the 20-km RUC using satellite and radar data. *14th Conf. on Num. Wea. Pred.*, Fort Lauderdale, FL, Amer. Meteor. Soc., J113-J115.
- Kim, D., and S.G. Benjamin, 2000: An initial RUC cloud analysis assimilating GOES cloud-top data. Preprints, 9th Conf. on Aviation, Range, and Aerospace Meteorology, AMS, Orlando, 522-524.
- Lynch, P. and X.-Y. Huang, 1992: Initialization of the HIRLAM model using a digital filter. *Mon. Wea. Rev.*, **120**, 1019-1034.
- Pan, H.-L. and L. Mahrt, 1987: Interaction between soil hydrology and boundary-layer development. *Bound.-Layer Meteorol.*, **38**, 185-202.
- Olsen, M.A., W.A. Gallus, J.L. Stanford, and J.M. Brown, 2000: An intense Midwestern cyclone: Fine-scale comparisons of model analysis with TOMS total ozone data. *J. Geophys. Res.*, **105**, 20487-20495.
- Pan, Z., S.G. Benjamin, J.M. Brown, and T. Smirnova, 1994: Comparative experiments with MAPS on different parameterization schemes for surface moisture flux and boundary-layer processes. *Mon. Wea. Rev.*, **122**, 449-470.
- Peters-Lidard, C. D., E. Blackburn, X. Liang, and E. F. Wood, 1998: The effect of soil thermal conductivity parameterization on surface energy fluxes and temperatures, *J. Atmos. Sci.*, **55**, 1209-1224.
- Reisner, J., R.M. Rasmussen, and R.T. Bruintjes, 1998: Explicit forecasting of supercooled liquid water in winter storms using the MM5 mesoscale model. *Quart. J. Roy. Meteor. Soc.*, **142**, 1071-1107.
- Schreiner, A. J., T. J. Schmit, W. Paul Menzel, 2001: Clouds based on GOES sounder data. *J. Geophys. Res.*, **106**, (D17), 20349-20363.
- Schwartz, B.E., and S.G. Benjamin, 2002: Verification of RUC surface forecasts at major U.S. airport hubs. *10th Conf. on Aviation, Range, and Aerospace Meteorology*, Portland, OR, Amer. Meteor. Soc., 327-330. (available in PDF from <http://ruc.fsl.noaa.gov> under 'RUC pubs')
- Smirnova, T.G., S.G. Benjamin, and J.M. Brown, 2000: Case study verification of RUC/MAPS fog and visibility forecasts. *9th Conf. on Aviation, Range, and Aerospace Meteorology*, AMS, Orlando, 31-36.
- Smirnova, T.G., J.M. Brown, S.G. Benjamin, and D. Kim, 2000: Parameterization of cold-season processes in the MAPS land-surface scheme. *J. Geophys. Res.*, **105**, D3, 4077-4086.
- Smirnova, T. G., J. M. Brown, and S. G. Benjamin, 1997: Performance of different soil model configurations in simulating ground surface temperature and surface fluxes. *Mon. Wea. Rev.*, **125**, 1870-1884.
- Smith, T.L., and S.G. Benjamin, 2002: Visibility forecasts from the RUC20. *10th Conf. on Aviation, Range, and Aerospace Meteorology*, Portland, OR, Amer. Meteor. Soc., 150-153. (available in PDF from <http://ruc.fsl.noaa.gov> under 'RUC pubs')
- Smolarkiewicz, P.K., 1983: A simple positive-definite advection transport algorithm. *Mon. Wea. Rev.*, **111**, 479-486.



#### **APPENDIX A. Known or suspected RUC20 biases or deficiencies as of April 2002 (per FSL)**

- Some remaining light precipitation bias. Even though the RUC20 clearly has reduced the dry precipitation bias from the RUC40, some of this bias remains (Fig. 7).
- Weak diurnal cycle. Again, this problem has been considerably improved in the RUC20, but it has not disappeared. The RUC20 seems to do fairly well for daytime temperatures, but overall, does not cool quite enough at night (Fig. 8).
- Too cold at night over snow cover. The RUC20 seems to cool off at night too much over snow covered areas. FSL has developed a fix to this problem that will be tested further and, if successful, will be implemented hopefully over the next several months.



## **APPENDIX B. Comments from field users during RUC20 evaluation from late March to early April 2002.**

*Fred Mosher – SOO – Aviation Weather Center*

While the time period for the RUC20 evaluation was short, and the weather was rather benign during the evaluation period, the evaluation did show the RUC20 to be a definite improvement over the current RUC2 model. The AWC evaluation focused mainly on the derived hazard fields (clouds, convection, turbulence, and visibility) rather than the traditional state of the atmosphere parameters (winds, temperature, etc.). The cloud tops and the convective cloud tops showed a major improvement, as did the visibility fields. This shows a definite improvement in the moisture distribution and the cloud physics parameterizations within the models, as well as the ability of the RUC20 to better assimilate initial time period meteorological information. We did not notice any degradation of the forecast skill for any field, and we did notice big improvements in some fields. Hence the AWC would recommend that the RUC20 model become the operational NCEP model used for short-term forecasts.

*Steve Weiss – SOO – Storm Prediction Center*

Our ability to assess the RUC20 has been tempered somewhat by the relatively inactive severe weather season so far this spring, however we have been able to formulate some preliminary assessments based on a small number of cases so far. I will focus on the Mar 25, Mar 29, and Apr 2 severe weather cases and attach some gif images relevant to each case. In the gif images [not shown here], the RUC40x files refer to the RUC20 output displayed on a 40 km grid. In addition, Greg Carbin has created two web pages that examine 1) a 3 hour forecast of precipitation valid at 00z Mar 18, and 2) 06z 28 Mar 00hr forecasts of 850 mb wind associated with the low level jet. These can be found at <http://www.spc.noaa.gov/staff/carbin/rucrvu/> and <http://www.spc.noaa.gov/staff/carbin/rucrvu2/>.

In Greg's first case, the RUC20 appears to overforecast the development of a precipitation along a front across the TN valley into AR, with radar showing that an elevated band of convection north of the front (and RUC20 forecast) is the primary precipitation activity at the verifying time. In his second case, he observed that the RUC20 depicts 850 mb winds that are much weaker than observed by profilers and radar VWP. (There is some question regarding a possible influence of birds and/or insects in the profiler/VAD winds, especially near the center of the 850 mb low where you might expect weaker winds.) In both cases, the RUC40 appeared to be better than the RUC20. If you have the data available, it would be good to look back at these cases. [FSL note: This case is a bird contamination flagging issue. The RUC40 does not use the Profiler Hub flags, and so it let through profiler observations that the RUC20 did not use since it honors the Profiler Hub flags.]

Our assessment focus has been primarily on short range forecasts of moisture, instability, and precipitation in support of our short range severe weather forecast mission. Overall, we have found no persistent evidence suggesting that the RUC20 should not be implemented as scheduled on April 16. The higher model resolution in the RUC20 seems to develop mesoscale features in the precipitation and vertical velocity fields that appear more realistic than the RUC40, even when viewed at identical display resolutions. In addition, our small sample indicates the forecasts of MUCAPE are better from the RUC20 than the RUC40, although aspects of low level temperature and dew point profiles from one case (Mar 29) raise interesting questions concerning the evolution of the afternoon boundary layer. Given the small number of cases we have seen, we plan to continue evaluating the RUC20 during this storm season in order to gain a better understanding of its strengths and weaknesses as it relates to convective forecasting issues. As always, we appreciate the opportunity to participate in the pre-implementation evaluation.

Mar 25...15z runs with forecasts valid at 00z and 03z

A weak surface low was forecast to move into central AR during the afternoon, and both RUC20 and RUC40 showed a similar scenario that verified well by 00z. The RUC20 predicted higher CAPE into central AR compared to the RUC40 (1000-1500 j/kg versus around 500 j/kg) and the stronger CAPE forecast also verified better. Both RUC versions predicted 3 hourly precipitation developing near the front from western TN across AR into parts of LA and east TX by 00z and continuing through 03z. Although precipitation did develop along the corridor predicted, both models were too fast in developing storms southward into east TX. The RUC20 700-500 mb mean



vertical velocity and 3 hourly precipitation forecasts exhibited more detailed structures that appeared to relate better to the actual convective development when compared to the RUC40 forecasts.

Mar 29...12z runs with forecasts valid 00z

On this day, there were two severe threat areas: 1) morning elevated severe storms moving eastward from MO toward the OH valley were expected to develop southward into the warm sector over AR/TN during the afternoon, and 2) new convection was expected to develop over west/north central TX during the late afternoon or evening as moisture returned northwestward across TX in advance of a strong upper low moving toward the southern Rockies.

Both models were similar in predicting surface dew points over the lower MS valley region although the 12 hour forecast from the RUC20 was considered slightly better. Across TX both models did not transport surface moisture fast enough into southwest and central TX, with the RUC40 worse than the RUC20. This resulted in not enough instability being forecast into central and southwest TX by both models. Overall, the instability predicted over the lower MS valley region by the RUC20 was "in the ballpark", and better than that from the RUC40 (see below for more discussion of sounding profiles).

Twelve-hour forecasts of 3 hourly precipitation were similar from both models but the RUC20 showed more realistic details in structure and location when compared to observed radar images over the OH and lower TN valleys. Unlike the RUC40, the RUC20 also developed precipitation over a small part of southwest TX by 00z. Although deficient in coverage, the RUC20 forecast was more in agreement with the severe storms that had developed by that time over parts of southwest/west central TX.

We also looked closely at model forecast soundings constructed from 25 mb vertical grids, and compared the model forecasts with observed soundings at LIT, SHV, and JAN. (There was precipitation occurring at BNA by 00z, so this sounding may not be representative of the preconvective environment.) In all cases, the models were able to accurately predict the general vertical structure in the warm sector showing a warm, moist boundary layer overlaid by an inversion based in the 800-850 mb layer, with drier conditions above the inversion before moistening again in the middle and upper levels. The forecast inversion was not as sharp as in the observed soundings, but this may be partially related to the use of 25 mb vertical grids which can smooth out some of the details between vertical levels. In all cases the RUC20 appeared to produce a boundary layer that was cooler and more moist than the observed boundary layers. The RUC40 forecast soundings were characterized by low level temperature profiles similar to observed profiles, but moisture was greater than forecast (similar to the RUC20). As a result, the RUC20 moisture/temperature errors tended to compensate for each other and forecast MUCAPE values were closer to the observed values, whereas the RUC40 MUCAPE values were much higher than observed. Here is a small table with forecast and observed MUCAPE values from two raob sites at 00z 30 Mar computed from NSHARP:

Location	RUC20	RUC40	Raob
SHV	2303	3869	2831
LIT	2708	3541	1879

(JAN observed sounding was a short run – observed MUCAPE could not be computed)

Apr 02...12z run with forecasts valid 00z

There was a slight risk of severe thunderstorms across parts of AR/west TN in the day 2 and day 1 outlooks. Moisture was forecast to return northward ahead of an advancing cold front, with an axis of instability forecast by the RUC40 and RUC20 during the afternoon. A primary question was determining whether or not thunderstorms would develop along the front during the afternoon. Both versions of the RUC indicated little in the way of precipitation by 00z, although the RUC20 showed a better defined axis of upward vertical motion in the 700-500 mb layer north of the surface front location. The lack of precipitation verified quite well, as thunderstorms failed to develop across the area. In this case, the forecast soundings were quite close to the observed sounding at LIT, including boundary layer profiles of temperature and moisture.



*Tim Garner – NWS Spaceflight Meteorology Group (SMG), Johnson Space Flight Center, Houston, TX*

I filled out the on-line form concerning the RUC for a forecast on 25 March for the Edwards AFB and White Sands areas. The RUC20 properly simulated that the mountains east of White Sands would block the progress of a cold front. Low level winds on either side of the Tularosa Basin (location of White Sands) were simulated quite well. Flow inside the basin during the day was quite light and variable so it was hard to ascertain how well the model performed. In general that day it did an admirable job simulating the low level winds in southern California.

I looked in more detail on the 27th when I used the 06Z and 12Z RUC20 runs as the primary tool for a landing simulation that we were working. The RUC20 appeared to be the only model (including NGM and AVN MOS) that forecasted a sea breeze in Florida. The forecast verified quite well. I had to fend off a lot of questions from some of the NASA users as to whether or not I was sure the winds would change. The RUC20 was almost spot on with the 10m winds. It did seem to overdo the precipitation in Florida later that afternoon, but I didn't stick around much after 21Z to see how well it did. This is a great improvement. I remember how poorly the RUC low level winds were over Florida when it first came out. The early RUC was so disappointing that we lost so much confidence in it that we rarely used it.

As far as precipitation forecasts go, neither Tim Oram nor I have noticed whether it has been any better or worse than the RUC40.

*Pablo Santos – SOO, Miami, FL*

We have been using the model operationally for almost two weeks. Weather has been quite active for us particularly during the afternoons this whole week. I used the model myself operationally for two days last week and I have gotten feedback from 2 forecasters so far. So far the model is proving to be a very good mesoscale guidance tool. It picks up the sea breeze development but not as well as the Eta 12 although we might attribute that to resolution [FSL note: Using 40km display] and the fact the we are looking at the Eta 12 in AWIPS through the D2D which gives us a lot of control over the display properties. The precipitation field forecast is turning out to be pretty good also although we do not concentrate much on QPF but rather the when and where. In this area it seems to be hand on hand with the Eta12. Although it is to early and soon to tell given how long we have had it, you can tell data from the FSL Mesoscale data networks is going into it, and hence FAWN (Florida Agricultural Weather Network) (am I right?). It seems it produces better analysis fields to begin with that guidance we obtain from NCEP. Again, this is something I cannot conclude for certain until I get the data in AWIPS and am able to sample to grid. [FSL note: Mesonet data is only assimilated in FSL RUC20 as of this time, but is planned to be added to the NCEP RUC20 within a few months of this writing.]

The great advantage with this model is how frequently it updates. It really provides us with an excellent tool in the scale of hours when rapidly developing/weakening Florida type convection occurs. That to us is invaluable.

*Chris Buonanno – SOO, Little Rock, AR*

Our office has often utilized the precipitation forecasts from the RUC20. We have found these forecasts to be particularly useful during the 6-18 h time frame, to help determine areal coverage (or lack of), and quantitative precipitation amounts during convective situations. We have noted that overall locations of forecast precipitation from the RUC20 seem to be improved compared to those from the RUC40. We have also noted during several recent events that the RUC20 correctly forecasted a lack of precipitation during situations where convective inhibition limited the extent of convection.